

KAUNAS UNIVERSITY OF TECHNOLOGY
FACULTY OF MECHANICAL ENGINEERING AND DESIGN

Oswald Vincent Joseph Arockia Raj

**ANALYSIS OF STRUCTURES WITH POLYMER BASE
PROTECTIVE COATINGS**

Final project for Master degree

Supervisor

Assoc. Prof. Dr. Kazimieras Juzenas

KAUNAS, 2015

KAUNAS UNIVERSITY OF TECHNOLOGY
FACULTY OF MECHANICAL ENGINEERING AND DESIGN

**ANALYSIS OF STRUCTURES WITH POLYMER BASE
PROTECTIVE COATINGS**

Final project for Master degree
Master of Science (621H30001)

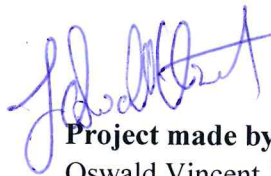
Supervisor

Assoc. Prof. Dr. Kazimieras Juzenas



Reviewer

Assoc. Prof. Dr. Paulius Griskevicius



Project made by

Oswald Vincent Joseph Arockia Raj

KAUNAS, 2015



KAUNAS UNIVERSITY OF TECHNOLOGY

Faculty of Mechanical Engineering and Design

(Faculty)

Oswald Vincent, Joseph Arockia Raj

(Student's name, surname)

Mechanical Engineering 621H30001

(Title and code of study programme)

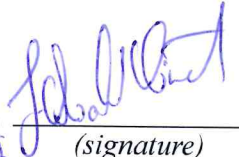
"Analysis of Structures with Polymer Base Protective Coatings" of final project

DECLARATION OF ACADEMIC HONESTY

12 June 2015
Kaunas

I confirm that a final project by me, **Oswald Vincent, Joseph Arockia Raj**, on the subject "Analysis of Structures with Polymer Base Protective Coatings" is written completely by myself; all provided data and research results are correct and obtained honestly. None of the parts of this thesis have been plagiarized from any printed or Internet sources, all direct and indirect quotations from other resources are indicated in literature references. No monetary amounts not provided for by law have been paid to anyone for this thesis.

I understand that in case of a resurfaced fact of dishonesty penalties will be applied to me according to the procedure effective at Kaunas University of Technology.

OSWALD VINCENT, JOSEPH AROCKIA RAJ 
(name and surname filled in by hand) (signature)

**KAUNAS UNIVERSITY OF TECHNOLOGY
FACULTY OF MECHANICAL ENGINEERING AND DESIGN**

Approved:

Head of Mechanical
engineering
Department

**MASTER STUDIES FINAL PROJECT TASK ASSIGNMENT
Study programme MECHANICAL ENGINEERING**

The final project of Master studies to gain the master qualification degree, is research or applied type project, for completion and defence of which 30 credits are assigned. The final project of the student must demonstrate the deepened and enlarged knowledge acquired in the main studies, also gained skills to formulate and solve an actual problem having limited and (or) contradictory information, independently conduct scientific or applied analysis and properly interpret data. By completing and defending the final project Master studies student must demonstrate the creativity, ability to apply fundamental knowledge, understanding of social and commercial environment, Legal Acts and financial possibilities, show the information search skills, ability to carry out the qualified analysis, use numerical methods, applied software, common information technologies and correct language, ability to formulate proper conclusions.

1. Title of the Project

Analysis of Structures with Polymer Base Protective Coatings

Approved by the Dean 2015 y. May m.11d. Order No. ST17-F-11-2

2. Aim of the project

Analysing the structures with polymer base protective coatings, by Finite Element Method

3. Structure of the project

A general introduction on failure of coatings, fracture mechanics techniques and delamination analysis is presented. A detailed description of Cohesive Zone Model is given along with its implementation in Finite Element Methods using ANSYS. Experimental procedures to obtain mechanical properties of coating is presented, which is used in model. CZM is used in analyzing Tensile Lap Shear according to ASTM D1002, which is further implemented in engineering structures to analyze delamination. CZM is found to be a reliable technique in analyzing delamination.

4. Requirements and conditions

General Requirement for Master Thesis

5. This task assignment is an integral part of the final project

6. Project submission deadline: 2015 June 1st.

Given to the student Oswald Vincent Joseph Arockia Raj

Task Assignment received Oswald Vincent Joseph Arockia Raj
(Name, Surname of the Student)

Supervisor Assoc. Prof. Dr. Kazimieras Juzenas
(Position, Name, Surname)


(Signature, date)

(Signature, date)

Joseph Arockia Raj, O.V. Analysis of Structure with Polymer Base Protective Coatings. *Master of Science* final project / supervisor Assoc. Prof. Dr. Kazimieras Juzenas; Kaunas University of Technology, Mechanical Engineering and Design faculty, Mechanical Engineering department.

Kaunas, 2015. 64 p.

SUMMARY

The aim of this work is to develop a novel Finite Element Model, to simulate the delamination of polymer based protective coatings. Coatings are used to enhance the life and performance of engineering equipment and components. A detailed study of existing techniques used in analysis of delamination is performed to find the best suitable method. The evaluation of delamination and adhesion strength in different loading conditions are simulated using ANSYS. Cohesive Zone Model (CZM), is used in modelling the interface between coating and substrate. The mechanical properties of coating, incorporated in the model, were obtained through laboratory experiments and manufacturer data sheets. Simulation model of Tensile Lap Shear is developed to analyse the reliability of model. Further this model is used in engineering structures to analyse delamination in real scenario. The results show delamination initiation at maximum normal contact stress and this ensures the reliability in results of model to be used in engineering structures. Subsequent investigations on effects of surface defects are performed in model, which simulates the real-time structures. These results can be used in optimization and enhancing coating properties. It can also predict the behaviour of coating in different loading conditions i.e. static loads, temperature loads, pressure loads and atmospheric loads. Future models can be developed to incorporate the effect of surface roughness on delamination.

Keywords: *Cohesive Zone Model, Delamination, Coatings, ANSYS*

Joseph Arockia Raj ,O.V. Konstrukcijų su polimero pagrindo apsauginėmis dangomis tyrimas. *Mechanikos inžinerijos* baigiamasis projektas / vadovas doc. dr. Kazimieras Juzėnas; Kauno technologijos universitetas, Mechanikos inžinerijos ir dizaino fakultetas, Mechanikos inžinerijos katedra.

Kaunas, 2015. 64 psl.

SANTRAUKA

Šio darbo tikslas yra ištirti naują baigtinių elementų modelį polimerų apsauginių dangų atsisluoksniavimui nustatyti. Tirtos dangos yra naudojama siekiant prailginti inžinerinės įrangos ir komponentų ilgaamžiškumą. Siekiant nustatyti tinkamiausius struktūrų su dangomis tyrimo metodus, atlikta esamų metodų analizė. Skaitiniams tyrimams naudojama ANSYS programa, kuri apskaičiuoja sukibimo jėgos ir atsisluoksniavimo sąlygas. Cohesive Zona Model (CZM) metodas yra naudojamas modeliuojant sąsają tarp dangos ir pagrindo. Į modelį įtraukos techninės dangos savybės buvo gautos laboratorinių eksperimentų metu ir buvo pateiktos gamintojo duomenų aprašuose. Etapinis tempimo šlyties metodas yra sukurtas nustatyti modelio patikimumui. Taip pat šis modelis yra pritaikomas analizuojant inžinerinių konstrukcijų atsisluoksniavimą. Atsižvelgiant į rezultatus, didžiausio kontaktinio slėgio zonoje prasideda atsisluoksniavimas. Tai pagrindžia modeliavimo metodo patikimumą. Tolimesniuose tyrimuose analizuojamas paviršinių defektų poveikis. Šie rezultatai gali būti naudojami optimizuojant polimerinėmis dangomis dengtas konstrukcijas. Taip pat tai leidžia nuspėti dangos elgseną esant skirtingoms apkrovos sąlygoms. Toliau tyrimai gali būti vykdomi analizuojant paviršiaus šiurkštumo įtaką atsisluoksniavimui.

Raktiniai žodžiai: *Cohesive Zona Model, atsisluoksniavimas, dangos, Ansys*

Table of Contents

Introduction.....	5
1.0 Delamination Analysis – Concepts.....	7
1.1 Linear Elastic Fracture Mechanics.....	8
1.3 Fracture Modes.....	12
1.4 Stress Analysis of Cracks.....	13
1.5 Stress Intensity Factor.....	14
1.6 Fracture in Polymers.....	15
1.6.1 Shear Yielding and Crazeing.....	15
1.7 Review on Analysis of Delamination.....	16
1.8 Delamination Propagation.....	18
1.9 Cohesive Zone Modelling.....	21
1.10 Standard Test Methods for Delamination.....	23
1.10.1 DCB Test.....	23
1.10.2 ENF Testing.....	24
2.0 Cohesive Zone Modelling with ANSYS.....	26
2.1 Interface Elements.....	26
2.1.1 Contact Elements.....	27
2.2 Debonding Modes.....	28
2.3 Material Model – Bilinear Behaviour.....	31
2.4 Defining Debonding.....	32
3.0 Implementation of Cohesive Zone Model.....	37
3.1 Obtaining Material Properties.....	37
3.2 Modelling Tensile Shear.....	41
3.2.1 Simulation Procedure.....	42
3.2.2 Results.....	44
3.2.3 Discussion.....	46

3.4 Delamination in Pipe Structures.....	47
3.5 Analysis of Surface Defects	54
4.1 Conclusion and Discussions.....	57
4.2 Future Work.....	58
References.....	59

List of Figures

Fig 1.0: Beam- Type Delamination Specimens	7
Fig 1.1: Potential Energy And Force As A Function Of Atomic Separation	9
Fig 1.2.: Coordinate System And Integration Contour For The J Integral	12
Fig1.3: Load Cases In Fracture Mechanics.....	13
Fig1.4: Definition Of The Coordinate Axis Ahead Of A Crack Tip	14
Fig1.8: Stress-Displacement Curve For (A) Ductile And (B) Brittle Separation	21
Fig1.9: Cohesive Zone Model.....	23
Fig1.10a: DCB Specimen	24
Fig1.10b: ENF Specimen.....	24
Fig2.1: INTER204 – 16node Cohesive Element	27
Fig2.1: Material Model – Bilinear Behaviour.....	28
Fig2.5: Newton-Raphson Solution – One Iteration	33
Fig3.2: 3-Point Bending Test Of Coating	38
Fig3.2a: Load – Displacement Curve Material 1	38
Fig3.2b: Load – Displacement Curve Material 2.....	39
Fig3.2c: Load – Displacement Curve Material 3	40
Fig3.2: Configuration Of Tensile Shear Model	41
Fig3.2a: Maximum Shear Stress Distribution-Entire Model	44
Fig3.2c: Max. Shear Stress Distribution - Coating.....	45
Fig3.2d: Contact Pressure - Coating	45
Fig3.2e: Shear Stress – Deformation Plot.....	46
Fig3.2f: Normal Stress – Deformation Plot - Coating	47
Fig3.4: Section Of Pipe With External Coating-Scheme.....	48
Fig3.4a: Normal Stress Distribution – Coating.....	50
Fig3.4b: Contact Gap - Coating	50
Fig3.4c: Pipe-Normal Stress-Normal Strain Plot.....	51
Fig3.4a: Pipe With Internal Coating-Scheme	52
Fig 3.4b: von-Mises Stress Distribution	52
Fig 3.4c: Normal Stress Distribution	53
Fig 3.4d: Normal Stress-Normal Strain	54
Fig 3.5a: Analysis Of Surface Defects On Coating - Scheme	55
Fig 3.5b: von-Mises Stress Distribution - Substrate	55
Fig 3.5c: Normal Stress Distribution - Coating	56

List of Tables

Table 2.3: Description Of Bilinear Material Behaviour With Traction And Separation Distances.....	31
Table 2.3: Description Of Bilinear Material Behaviour With Traction And Critical Fracture Energies	32
Table 3.2a: Material Properties – Structural Steel	42
Table 3.2b: Material Properties - Coating.....	42
Table 3.2c: Cohesive Zone Model - Parameters	43
Table 3.4a: Material Properties – Carbon Steel	49
Table 3.4b: Material Properties - Czm.....	49
Table 3.5: Material Properties – 6061 Aluminium Alloy	54

Introduction

Polymers are used in a various applications, like transport vehicles, sports equipment and various engineering applications like electronic equipment and protective coatings. These materials are susceptible to damage induced by mechanical, chemical, thermal, UV radiation of combination these factors. This could affect the properties of the material which will eventually reduce the performance of the materials. It may result in defects like micro crack which will eventually result in delamination, which will propagate and will affect the structural integrity of material.

Improving the performance of existing machinery and manufactured components is of a major economic importance. In the recent years, the growth of surface coatings is tremendous which improves wear resistance, reduce friction and improves life of metallic and metal based components. Coatings are being developed for specific problems which helps in improving performance of particular equipment ^[1]. The functioning of coating also depends on various parameters like surface preparation, surface roughness, application methods, drying time and type of load acting on the coating.

This work is aimed in analysing the structures with polymer base protective coatings, by Finite Element Method

1. Identification of an efficient technique to analyse delamination
2. Implementation of identified technique in Finite Element Model to analyse delamination
3. Applying the identified technique in engineering structures to study the behaviour of coating

A detailed survey on the methods of evaluating coating performance and strength has been done which introduced to classic methods like scratch test, pin-on-disc test and tape test. New techniques involving Finite Element Methods are also being used to analyse and improve coating performance. Linear Elastic Fracture Mechanics (LEFM) and Extended Finite Element Methods (XFEM) are also used to analyse exploitation of coatings. A specific method of LEFM is chosen in analysing the delamination of coatings.

A linear FEA can analyse the critical stress or strain, at which the failure occurs. After occurrence of failure the distribution of load is varied, which propagates the failure. This phenomenon is predicted by Fracture Mechanics techniques ^[2]. The Cohesive Zone Model

describes the fracture process more realistically ^[3]. The CZM is used to define and simulate the contact between substrate and coating. Contact element based delamination is implemented to analyse the adhesion strength of coatings.

Models to measure the strength of coating and its stress distribution is analysed using ANSYS. Material properties for the coating was obtained through bending tests in laboratory. The properties are used in developing the coating material for Finite Element Model. The CZM layer with zero thickness is used to simulate the bonding of coating and substrate. During deformation, the stiffness matrix of the bonding layer is updated with every iteration, which eventually becomes zero. This results in delamination of a particular node.

This approach is applied to various real engineering structures, which simulates the model in practical applications, which included different kinds of loading. Small surface defects and irregularities are also included to study the behaviour of model on irregular surfaces. Stress concentrations are observed in the vicinity of defects which results in delamination of coating. The factor of surface roughness is not included in this, which can be explored in future works.

Coatings are extensively used in various applications like water storage tanks, lift screws, impellers of pumps, conveyors – Screw conveyors, Bucket Conveyors etc., corrosion protection systems and pressure vessels. Delamination is a common issue to all kinds of applications which is one of the important failure that affects the performance. The approach suggested in this work can fulfil the requirements in analysis of coatings in various applications.

This report is further divided into five chapters, which includes a short Introduction, which gives a general idea of the work and method used. Secondly, a brief idea of concepts and review of existing and past researches, which gives a deep insight of previous works is included. This gives the basic idea of the entire work. Thirdly, a detailed description of the modelling is included. This will give introduction to Cohesive Zone Modelling concepts, models in which CZM is implemented. Fourth chapter, gives the application of CZM in analysing the tensile shear strength analysis and application in other models. Finally, Conclusion which gives a brief summary of the work and suggestions and improvements, that can be implement in modelling and practical cases to achieve better performance and results.

Chapter - 1

1.0 Delamination Analysis – Concepts

Delamination is a frequent mode of failure affecting the structural performance of coated structures. The interface between substrate and protective layer offers a low-resistance path for crack growth because the debonding between layers depends only on matrix properties [4]. Delamination can occur due to high concentrations of normal and shear stresses caused by geometrical effects, such as curved sections, sudden changes of cross-sections, and free edges, or from the mechanical, manufacturing, transportation and service effects, such as temperature, moisture and general loading conditions.

According to its shape, delaminations are classified into through-the-width or strip [5]-[9], circular [9, 10], elliptical [11], rectangular [12] or arbitrary [13, 14]. Other delamination configurations which have been investigated in the literature are the beam-type delamination specimens subjected to bending, axial and shear loading [15]-[21] which forms the basis for experimental methods used to measure the interlaminar fracture strength under pure mode I, mode II and mixed mode conditions in composites, adhesive joints and other laminated materials, Fig 1.

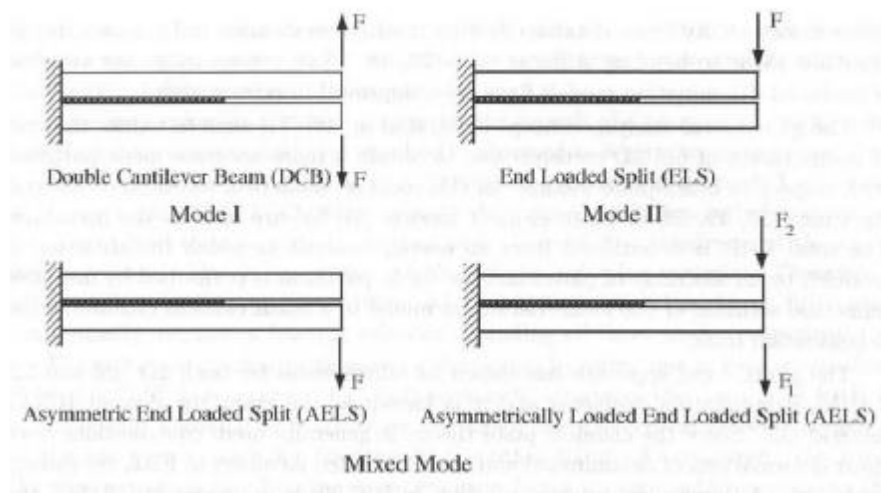


Fig 1.0: Beam- Type Delamination Specimens

Delaminations in layered plates and beams have been analysed by using different Finite Element Methods techniques, in which the results are not realistic. To overcome such inconsistency in results an approach using cohesive zone models and fracture mechanics is developed. A cohesive zone model implements interfacial constitutive law defined in terms of damage variables and a damage evolution law. The

cohesive zone elements are used between plane elements, solid elements, beam elements or shell elements ^[22]. A number of fracture mechanics-based models have been proposed in the literature to study delamination including three-dimensional models and simplified beam-like models ^[6].

1.1 Linear Elastic Fracture Mechanics

Fracture mechanics allows us to predict the growth of a pre-existing crack or defect. In a homogenous and isotropic body subjected to a generic loading condition, a crack tends to grow by kinking in a direction such that a pure mode I condition at its tip is maintained. On the contrary, delaminations in laminated structures are constrained to propagate in its own plane because the toughness of the interface is relatively low in comparison to that of the adjoining materials. Therefore a delamination crack propagates with its tip in mixed mode condition and consequently, required a fracture criterion including all three mode components.

A material fractures when sufficient stress and work are applied on the atomic level to break the bonds that hold atoms together. The bond strength is supplied by the attractive forces between atoms. A tensile force is required to increase the separation distance from the equilibrium value; this force must exceed the cohesive force to sever the bond completely. The bond energy is given by ^[39]

$$E_b = \int_{x_0}^{\infty} P dx$$

Where x_0 is the equilibrium spacing and P is the applied force. It is possible to estimate the cohesive strength at the atomic level by idealizing the interatomic force-displacement relationship as one half the period of a sine wave

$$P = P_c \sin(\pi \cdot x / \lambda)$$

Where the distance λ is defined in the fig 2. For sake of simplicity, the origin is defined at x_0 . For small displacements, the force-displacement relationship is linear

$$P = P_c (\pi \cdot x / \lambda)$$

And the bond stiffness (i.e., the spring constant) is given by $k = P_c \pi / \lambda$

Multiplying both sides of this equation by the number of bonds per unit area and the gauge length, x_0 , converts k to Young's modulus, E , and P_c to the cohesive stress, σ_c , solving for σ_c gives

$$\sigma_c = \frac{E\lambda}{\pi x_o} \text{ or } \approx \frac{E}{\pi}$$

If λ is assumed to be approximately equal to the atomic spacing.

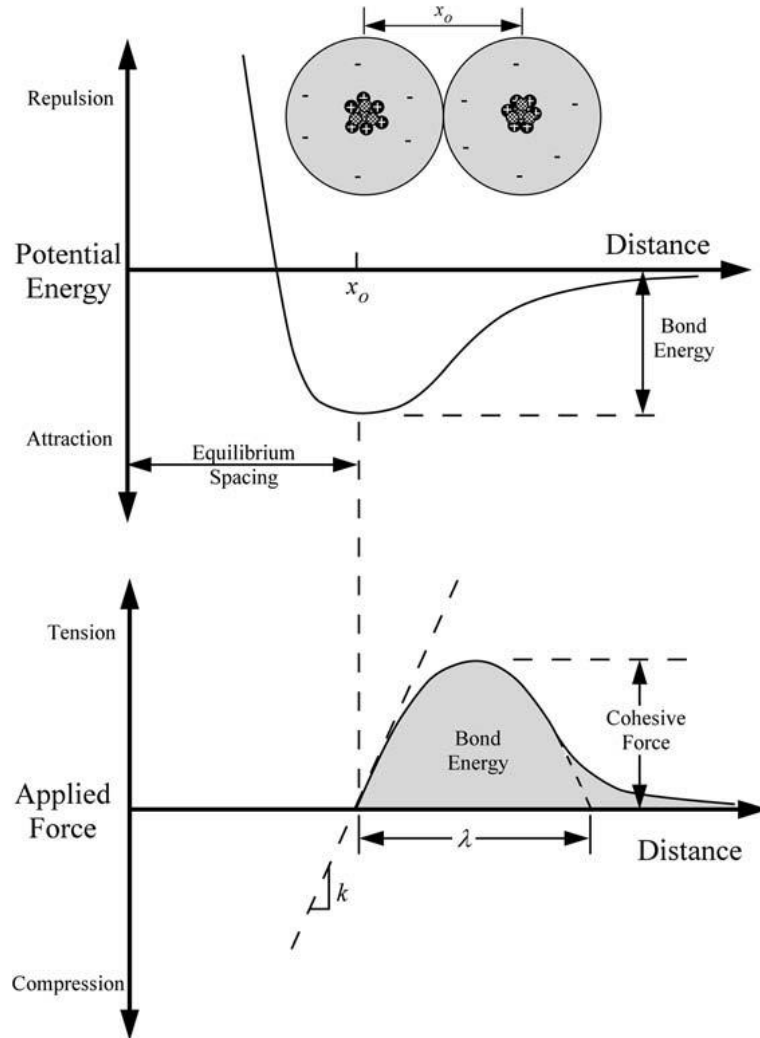


Fig 1.1: Potential energy and force as a function of atomic separation

[Courtesy: Fracture Mechanics, Fundamentals and Applications – T.L. Anderson]

Griffith Energy Balance

According to the First Law of thermodynamics, when a system goes from a non-equilibrium state to equilibrium, there will be a net decrease in energy. Griffith applied this idea to the formation of a crack as below [40]:

It may be supposed, for the present purpose, that the crack is formed by the sudden annihilation of the tractions acting on its surface. At the instant following this operation, the strains, and therefore the potential energy under consideration, have their

original values; but in general, the new state is not one of equilibrium. If it is not a state of equilibrium, then, by the theorem of minimum potential energy, the potential energy is reduced by the attainment of equilibrium; if it is a state of equilibrium the energy does not change.

A crack can form (or an existing crack can grow) only if such a process causes the total energy to decrease or remain constant. Thus the critical conditions for fracture can be defined as the point where crack growth occurs under equilibrium conditions, with no net change in total energy. By Griffith approach, fracture stress is given by

$$\sigma_f = \left(\frac{\pi E \gamma_s}{2(1 - \nu^2)a} \right)^{1/2}$$

Where E- Young's Modulus, γ_s – Surface energy of material, a- crack radius and ν – Poisson's ratio.

Modified Griffith Equation

Griffith fracture stress equation is valid only for ideally brittle solids. It is in good agreement between fracture stress equation and experimental fracture strength of glass, but Griffith equation severely underestimates the fracture strength of metals. Therefore, a modified Griffith expression to account for materials that are capable of plastic flow has been developed. The expression is as below ^[40]:

$$\sigma_f = \left(\frac{2E(\gamma_s + \gamma_p)}{\pi a} \right)^{1/2}$$

Where, γ_p is the plastic work per unit area of surface created, and is typically much larger than γ_s . In ideally brittle solid, a crack can be formed merely by breaking atomic bonds; γ_p reflects the total energy of broken bonds in a unit area. When a crack propagates through a metal, however, dislocation motion occurs in the vicinity of the crack tip, resulting in additional energy dissipation.

For metals, it is possible to generalize the Griffith model to account for any type of energy dissipation:

$$\sigma_f = \left(\frac{\pi E w_f}{\pi a} \right)^{1/2}$$

Where w_f is the fracture energy which could include plastic, viscoelastic, or viscoplastic effects, depending on the material. The fracture energy can also be influenced by crack meandering and branching, which increases the surface area. The Griffith model in particular applies only to linear elastic material behaviour. Thus the

global behaviour of the structure must be elastic. Any nonlinear effects, such as plasticity, must be confined to a small region near the crack tip.

Energy Release Rate

The energy approach is more convenient in solving engineering problems. The energy release rate G , which is the measure of energy available for an increment of crack extension ^[41]

$$G = \frac{d\Pi}{dA}$$

The potential energy of an elastic body, Π , is defined as

$$\Pi = U - F$$

Where U is the strain energy stored in the body and F is the work done by external forces.

The term rate, as it is used in context, does not refer to a derivative with respect to time; G is the rate of change in potential energy with the crack area. Since G is obtained from the derivative of a potential, it is also called the crack extension force or the crack driving force.

These basic laws and concepts help in formulation of micro analysis techniques that analyse cracks. It serves as a constitutive law to derive further methods which analyse failure more accurately.

1.2 Elastic-Plastic Fracture Mechanics

The linear-elastic fracture mechanics can only be used if the plastic zone near the crack tip is sufficiently small. While on the other case, the failure is in the domain of elastic-plastic fracture mechanics (EPFM) which can deal with a large plastic zone. The drawback of this method is, plastic behaviour must still be restricted to the region around the crack tip and must be mainly determined by the surrounding elastic stress field. Two methods describe the state near the crack tip are:

Crack tip opening displacement (CTOD)

The crack tip opening displacement, it is assumed that crack propagation is not determined by the stress intensity factor, but by the opening δt of the crack tip, if this reaches a critical value δc , the crack propagates.

J integral

The energy release rate technique quantifies the critical value G , it is independent of the material behaviour, and Linear-elastic behaviour was only assumed to calculate. The J integral can quantify the energy release rate without this assumption. For a crack geometry as in fig3, j is defined as

$$J = \int_C [w dx_2 - \left(\sigma \cdot \frac{\partial u}{\partial x_1} \right) \cdot n ds]$$

Here C is a closed curve encircling the crack tip, $w = \int \sigma_{ij} d\epsilon_{ij}$ is the energy density, u is the displacement vector and n , outwardly pointing normal vector on C .

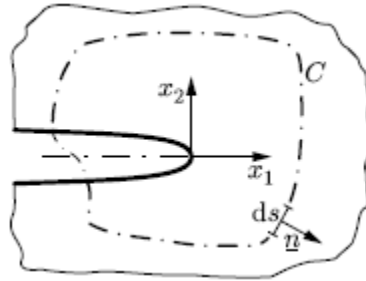


Fig 1.2.: Coordinate system and integration contour for the J integral

[Courtesy: Mechanical Behaviour of Engineering Materials – Joachim Roesler]

These techniques are used to analyse the propagation or stress concentration of an existing crack in a homogenous material. In practical application, the cracks develop during the deployment of a material and loads acting on it. The main disadvantage of these techniques is, they do not calculate the initiation of a crack. To analyse the crack initiation a better and realistic techniques like Cohesive Zone Model is used.

1.3 Fracture Modes

Three characteristic load cases are distinguished in fracture mechanics, which differ in the orientation of the stress field to crack. They are called mode I, mode II and Mode III. In mode I (Fig4-a), the largest principal stress σ_1 is oriented perpendicularly to the crack surface. Tensile stresses open the crack and thus separate the surface. Compressive stresses close the crack so that forces can be transmitted almost identically to a case without a crack. In Mode II (Fig 4-b) and mode III (Fig4-C), the crack surfaces are loaded in shear. These modes do not open the crack. When the load is applied, the crack surfaces slide with friction and thus dissipate part of the external work. Mixed-

mode loads can also occur. The energy dissipated in modes II or III is not available for crack propagation, a crack propagates at smaller loads in mode I. independent of its initial orientation, a growing crack thus changes its orientation to be perpendicular to the maximum principal stress i.e., to be loaded in mode I, if stress field and material are homogenous. This load case is therefore the most important one. The maximum principal stress σ_1 therefore determines the material behaviour in crack propagation.

When the crack propagated, the crack surface can be formed by either shear or cleavage fracture, or a mixture of both, leading to fracture surfaces. If fracture occurs by crack propagation at stresses below yield strength, the global plastic deformation of the component is usually small because plastic deformation is localised at the crack tip.

These are the general fracture modes found in materials. Pure fracture occurs in homogenous materials. A mixed mode fracture is a common failure observed in many applications. Delamination is a mixed mode fracture which propagates in its own plane.

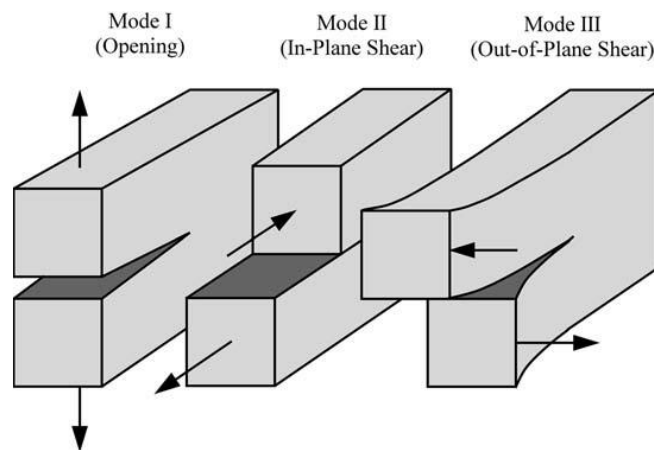


Fig1.3: Load cases in fracture mechanics

[Courtesy: Fracture Mechanics, Fundamentals and Applications – T.L. Anderson]

1.4 Stress Analysis of Cracks

The stress at the crack tip is analysed as a planes stress in polar coordinate system. For certain cracked configurations subjected to external forces, it is possible to derive closed-form expressions for the stresses in the body, assuming isotropic linear elastic material behaviour ^[44, 45]. If we define a polar coordinate axis with the origin at the crack tip it can be shown that the stress field in any linear elastic cracked body is given by

$$\sigma_{ij} = \left(\frac{k}{\sqrt{r}}\right) f_{ij}(\theta) + \sum_{m=0}^{\infty} A_m r^{\frac{m}{2}} g_{ij}^{(m)}(\theta)$$

Where σ_{ij} – stress tensor, r and θ –coordinates (Shown in Fig5) k -constant, f_{ij} - dimensionless function of θ in the leading term.

For the higher-order terms, A_m is the amplitude and $g_{ij}^{(m)}$ is a dimensionless function of θ for the m th term. The higher-order terms depend on geometry, but the solution for any given configuration contains a leading term that is proportional to $\frac{1}{\sqrt{r}}$. As $r \rightarrow 0$, the leading term approaches infinity, but the other terms remain finite or approach zero. Thus, stress near the crack tip varies, regardless of the configuration of the cracked body.

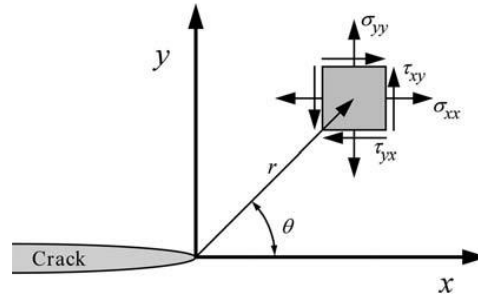


Fig1.4: Definition of the coordinate axis ahead of a crack tip
[Courtesy: Fracture Mechanics, Fundamentals and Applications – T.L. Anderson]

1.5 Stress Intensity Factor

Each mode of loading produces the $\frac{1}{\sqrt{r}}$ singularity at the crack tip, but the proportionality constants f_{ij} and k depend on the mode. This constant k is replaced by the stress intensity factor K , where $K = k\sqrt{2\pi}$. The stress intensity factor is usually given a subscript to denote the mode of loading i.e., K_I, K_{II}, K_{III} . Thus the stress field ahead of a crack tip in an isotropic linear elastic material is written as

$$\lim_{r \rightarrow 0} \sigma_{ij}^I = \frac{K_I}{\sqrt{2\pi r}} f_{ij}^I(\theta)$$

$$\lim_{r \rightarrow 0} \sigma_{ij}^{II} = \frac{K_{II}}{\sqrt{2\pi r}} f_{ij}^{II}(\theta)$$

$$\lim_{r \rightarrow 0} \sigma_{ij}^{III} = \frac{K_{III}}{\sqrt{2\pi r}} f_{ij}^{III}(\theta)$$

For modes I, II and III respectively. In a mixed-mode problem, the individual contributions to a given stress component are additive

$$\sigma_{ij}^{total} = \sigma_{ij}^I + \sigma_{ij}^{II} + \sigma_{ij}^{III}$$

Stress Intensity Factor determines the contribution of the failure mode in delamination or crack propagation. It is an important parameter in formulation of the model, modern simulation softwares are able to calculate the stress intensity factors themselves, while it still remains to the choice of user when defining the model.

1.6 Fracture in Polymers

The fracture behaviours of polymeric materials has only recently become a major concern, as engineering plastics have begun to appear in critical structural application. In metals, fracture and yielding are competing failure mechanisms. Brittle fracture occurs in materials in which yielding is difficult. Ductile metals, by definition, experience extensive plastic deformation before they eventually fracture. Low temperatures, high strain rates, and triaxial stresses tend to suppress yielding and favour brittle fracture.

Polymers do not contain crystallographic planes, dislocations, and grain boundaries; rather they consist of long molecular chains. A complicating feature for polymers, however, is that two types of bond govern the mechanical response: the covalent bonds between carbon atoms and the secondary van der Waals forces between molecule segments. Ultimate fracture normally requires breaking the latter, but the secondary bonds often play a major role in the deformation mechanisms that leads to fracture.

The factors that govern the toughness and ductility of polymers include the strain rate, temperature and molecular structure. At high rates or low temperatures polymers tend to be brittle, because there is insufficient time for the material to respond to stress with large-scale viscoelastic deformation or yielding. Highly cross-linked polymers are also incapable of large scale viscoelastic deformation.

1.6.1 Shear Yielding and Crazing

Shear yielding in polymers resembles plastic flow in metals, at least from a continuum mechanics viewpoint. Molecules slide with respect to one another when

subjected to a critical shear stress. Shear-yielding criteria can either be based on the maximum shear stress or the octahedral shear stress [42, 43]

$$\tau_{max} = \tau_o - \mu_s \sigma_m$$

Where σ_m is the hydrostatic stress and μ_s is a material constant that characterizes the sensitivity of the yield behaviour to σ_m when $\mu_s=0$ this equation reduces to the Tresca and von Mises yield criteria.

Glassy polymers subject to tensile loading often yield by crazing, which is a highly localized deformation that leads to cavitation and strains on the order of 100%. The craze zone usually forms perpendicular to the maximum principal normal stress. Fracture occurs in a craze zone when individual fibrils rupture. This process can be unstable if, when a fibril fails, the redistributed stress is sufficient to rupture one or more neighbouring fibrils.

Crazing is a major failure criteria in polymers experienced in the engineering industry. The delamination also initiates and propagates by crazing formation in the interface layer. Modelling crazing is quite complicated and requires high computation cost.

1.7 Review on Analysis of Delamination

Analysis of delamination can be classified into two main types: analytical and computational approaches. The first includes the analytical solutions for ideal cases of semi-infinite biomaterial problems, and comprises static and dynamic solutions for isotropic, orthotropic and functionally graded materials. The oscillatory near-tip behaviour for a traction-free interface crack between two dissimilar isotropic elastic materials [46]. Later, a violation was reported on the basic open-crack assumption by predicting potential interpenetration or overlapping of crack surfaces in biomaterials, which was an indication of the existence of a contact zone near the crack tip [47]. This contradiction was further studied by examining the stress singularities near the tip of an interfacial crack by assuming that the crack surfaces were in contact near the tip [48].

Derivation of bimaterial stress intensity factor K1 and K2 was performed based on the fundamental concepts of fracture mechanics [49]. Unlike the homogenous case. It is concluded that the individual stress intensity factors were not associated with the opening and shearing modes of fracture, respectively. As discussion on the total strain

energy release rate of an interfacial crack between isotropic solids and the non-existence of separable strain energy release rates for mode I (G_1) and mode II (G_2) due to their oscillatory natures ^[50].

The study of interface cracks was not limited to isotropic biomaterials and several other researches were done on interface crack between two anisotropic materials ^[51]. The mixed mode analysis of interface cracks in anisotropic materials was also carried out, while this led to discussions on biomaterial oscillatory index and its dependence on material orientations. A major step forward was by proving a necessary and sufficient non-oscillatory condition for separately defining the three fracture modes ^[52]. It also identified that the Irwin-type energy release rate was simply the average of the corresponding results for the two homogenous materials. Similar methodologies were used to evaluate mixed mode strain energy release rates and other fracture mechanics parameters for an interfacial crack between two orthotropic layers ^[53].

A stress-based approach has also been developed to assess the performance of debonded composite laminates and to discuss the potential delamination propagation ^[54]. In this approach, evaluation of the interfacial stress distribution is based on an elastic assumption and the delamination criterion is a simple comparison of the computed stress state with the adhesive strength. Linear elastic theory is used to derive shear and peeling stresses and to calculate the critical stress levels at the end of an outer reinforcement plate ^[55]. The analysis of composite beams with partial interaction and proposed models for interface shear stress concentration near the ends of the epoxy-bonded external plates are also proposed.

In the second category of analysis of bimaterial interface cracks and delamination, a vast variety of computational techniques have been adopted for analysis of multilayer orthotropic composites and the study of interlaminar crack stability and propagation. The finite element method (FEM), which has been the basis for many studies of fracture mechanics related problems, including fracture, unless a better solution is proposed. In addition, the boundary element method (BEM), the discrete element method (DEM) ^[56], meshless methods such as the element-free Galerkin method (EFG) ^[57] and the meshless local Petrov-Galerkin approach (MLPG), the extended finite element method (XFEM) and the extended isogeometric analysis (XIGA) ^[58] are probably the main classes of computational techniques that are currently

available for efficient analysis of various crack problems, including interface cracks and delamination problems.

Most of the performed numerical simulations prior to the end of twentieth century were related to the finite element method. Interlaminar crack simulation in FEM has been performed with a number of assumptions on the way a crack is represented. They mainly include continuous smeared crack models, discrete inter-element crack models, cracked interface elements and the discrete element used approach, which may use general contact mechanics algorithms to simulate progressive delamination and fracture problems ^[56]. These models may represent a cohesive interface approach, which employs a layer of interface elements ^[59] or a general contact interface between the materials to analyse partially delaminated layered composites ^[60].

On the other hand, a large number of studies have used computationally evaluated fracture mechanics parameters, such as the stress intensity factors, the energy release rate or the J integral, in comparison with the relevant critical values to assess the crack stability. For instance, the initiation and propagation of the delamination, based on this concept, occurs if the amount of energy released by the system due to an infinitesimal crack growth is larger than the specific fracture energy of the material ^[61]. Most of the existing FEM-based LEFM debonding analysis differ mainly in the way the fracture mechanics parameters are evaluated. A high-order theory for the stress analysis of the FRP-strengthened beam, in combination with the J integral formulation or numerical differentiation of the total potential energy, for evaluation of the energy release rate has been done ^[62].

The above computational and analytical techniques are used to evaluate an existing crack or a premeshed crack in the model. The advanced computational models such as BEM, DEM and XFEM require high storage memory. The memory requirement is linear to the complexity of the problem analysed and hence these methods are not practically possible to use in engineering analysis. The

1.8 Delamination Propagation

1.8.1 Fracture Energy-Based Criteria

The state of stability of a 2D interlaminar crack can be examined by a mixed mode criterion in terms of the fracture energy release rate G and the corresponding critical value

$$(G_I/G_{Ic})^{m/2} + (G_{II}/G_{IIc})^{m/2} = 1$$

Various values for the parameters m and n haven proposed, based on test data curve fitting techniques [63]. There is usually no need for any specific crack propagation criteria to determine the angle of crack propagation for 2D interlaminar cracks; predefined interface cracks are generally assumed to propagate along the interface. Therefore, once the stability of an interface crack is violated, the interlaminar crack can be assumed to self-similarly propagate in a quasi-static manner. For dynamic problems, however, the extent of delamination can be determined from the crack-tip velocity and the analysis time-step.

1.8.2 Stress-Based Criteria

The simple Chang-Springer based criterion has been frequently used for prediction of the initiation or propagation of delamination in 3D problems.

$$\frac{\sigma_n^2}{S_n^2} + \frac{\sigma_{t1}^2 + \sigma_{t2}^2}{S_t^2} = 1$$

Where S_n and S_t are the unidirectional normal and tangential bonding strengths, respectively, σ represents the stress components normal to the interface σ_{t1} and σ_{t2} are the two orthogonal tangential stress components on the tangential interface plane.

The Hashin delamination criterion is based on the Change-Springer approach combine with a linear softening law. The delamination function can be defined as,

$$F(\sigma, a) = f(\sigma) - S_n(\eta) \leq 1$$

Where $f(\sigma) = \sqrt{\sigma^T A \sigma}$ and

$S_n(\eta) = S_{n0}(1 - \mu\eta)$, with

$$A = \text{diag}\left[1 \quad \frac{S_n^2}{S_t^2} \quad \frac{S_n^2}{S_t^2}\right]$$

η can be assumed as the equivalent strain and μ describes the slope of the softening curve $S_n(\eta)$ which can be determined from the critical energy release rate G_c , the initial tensile strength S_{n0} and the characteristic thickness of the bonding layer h_t

$$\mu = \frac{S_{n0}h_t}{2G_c}$$

Then, the rate of the internal variable can be determined from an evolution law

$$\dot{\eta} = \lambda \frac{\partial F(\sigma, \eta)}{\partial S_n}$$

Where λ is the proportionality constant.

1.8.3 Contact-Based Criteria

A number of delamination criteria have been proposed, based on the use of a contact interaction approach for simulation of interlaminar behaviour. The Chang-Springer criterion can also be regarded in this category if σ_n and σ_t stress components are assumed as the contact interlaminar stresses. Assumptions for interaction between normal and tangential fracture modes, especially in the softening regime, have resulted in a number of delamination criteria. Such an interaction is usually quantified by a variable k in terms of the ratios of the normal and tangential relative displacements of the interface, g_n and g_t respectively

$$k = \left\{ \left(\frac{g_n}{g_n^{max}} \right)^a + \left(\frac{g_t}{g_t^{max}} \right)^a \right\}^{1/a} - 1$$

Where g_n^{max} and g_t^{max} are the maximum tolerable relative displacements in the normal and tangential directions, respectively. α is a constant variable between 2 and 4. The general methodology is usually designed on the basis of defining normal and tangential stress components of the interface for loading and unloading conditions based on the existing relative displacements g_n and g_t , maximum tolerable values of g_n^{max} and g_t^{max} and an assumption for the dependence of the energy release rate G , the variable k and the strength S_n .

Whichever modelling method is used in delamination analysis, the key element is the presence of a work of a separation or fracture energy. This parameter governs delamination initiation and growth, in addition to the tensile strength. It is defined as the work needed to create a unit area of fully developed crack.

$$G_c = \int_{u=0}^{\infty} \sigma du$$

Where σ and u are the stress and displacement respectively, across the fracture process zone. It is equal to the area under the decohesion curve (Fig6).

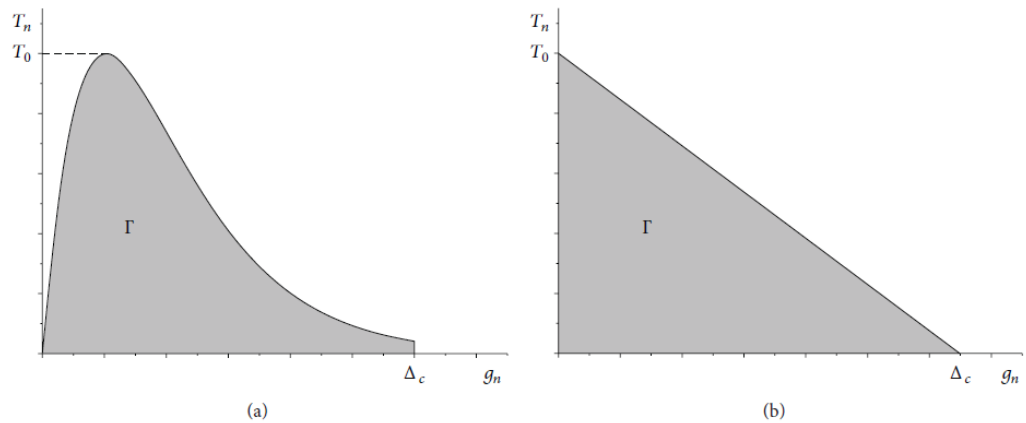


Fig1.8: Stress-Displacement Curve for (a) Ductile and (b) Brittle separation

These analysis criteria calculate the delamination stress and separation distances. This methods are used in ANSYS delamination analysis. ANSYS has a combined model of stress and contact based criteria. A separate model is available for energy based criteria. It is quite simple to use contact and stress based criteria as it can be adapted to an existing contact problem, without any changes in model.

1.9 Cohesive Zone Modelling

Cohesive zone concept is intended to describe the fracture process more realistically, such that the stress singularities, found in LEFM, do not arise [25]. Cohesive Zone Models have been extensively used for non-linear incremental analysis of interface debonding in few literatures [22, 23]. Unlike other methods that are directly based on fracture mechanics, they do not require the presence of an initial crack, can be more easily coupled with other material and geometric nonlinearities and allow for efficient implementations in a finite element setting via interface elements. Their use is often limited by the requirement for a very refined mesh around the process zone and because of the strongly nonlinear structural response, which might be difficult to follow even by using sophisticated path-following techniques [24].

The idea of cohesive zone model can be traced to the strip yield models [25, 26]. In this way, the unrealistic continuum mechanics stress singularity at the crack tip can be avoided. Several merits make the cohesive zone model popular in fracture mechanics. It seems to mimic many process zone effects in engineering materials. The fracture process, isolated from surrounding continuum constitutive material, is very

simple: traction versus separation. It is easy to implement the cohesive zone model in the finite element method using interface elements or contact elements. The cohesive zone model has been successfully used in solving the complicated fracture problems such as mixed mode fracture ^[27], fatigue fracture ^[28, 29] and dynamic fracture ^[30, 31].

At propagation stage of a crack, a fracture process zone exists in front of the crack tip, where microvoids initiate, grow, and finally coalesce with the main crack. The material behaviour in this fracture process zone is completely different from that of the surrounding bulk material. The conventional elastic-plastic constitutive relation used in bulk material is not suitable for this local material degraded region. When formulating analytic solutions to problems involving the fracture process zone, a new constitutive relation is necessary. Compared with the other characteristic dimensions of the region, the thickness of the fracture process zone is very small. Therefore, it is reasonable to assume that the fracture process zone which is subjected to cohesive traction forces, which will be completely absent in case of no load. In this case, the fracture process zone is termed as cohesive zone which consists of two fictitious cohesive surfaces. The traction separation law describes the relation between traction force in cohesive zone and its corresponding displacement. In contrast to the standard concept in continuum mechanics, CZM allows for a displacement jump inside the material and for separation of cohesive surfaces which finally leads to failure of the material. CZM categorises the material properties into two parts: deformation and separation. For the bulk material, deformation is accounted by continuum material model, on the other hand, fracture zone is modelled with the traction separation law.

The choice of a constitutive law for the cohesive zone is the most delicate aspect of this approach to fracture mechanics. Due to the small scale of the cohesive zone in most materials, it is experimentally quite difficult to determine the precise nature of the constitutive behaviour in the cohesive zone. This, it has become commonplace to postulate a phenomenological form for the cohesive zone model is mainly based on the fracture characteristic of the material, for example, ductile or brittle modes. In the literature, several cohesive zone constitutive models can be found. Typical cohesive zone laws include linear decreasing form ^[32], cubic and exponential form ^[33, 34], constant form ^[35], bilinear form ^[36], trilinear form ^[37] and polynomial form ^[38].

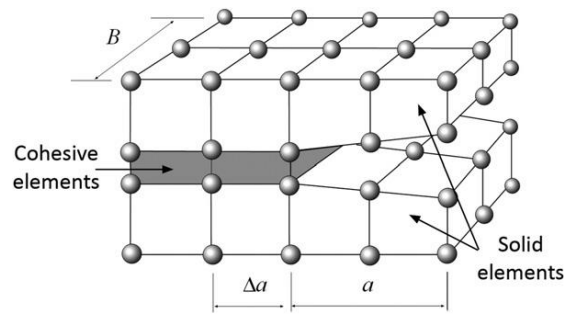


Fig1.9: Cohesive Zone Model

Researches have been carried out in analysing the performance of various constitutive relations. The comparison between polynomial and exponential damage curves has proven difference in the load-deflection curves ^[23]. The chosen comparison parameters were stiffness, fracture energy and peak stress, this was analysed and compared in mixed-mode loading case. Also great amount of research is being carried out in standardizing the model for both ductile and brittle material. It has been successfully developed by introducing a new parameter into conventional cohesive zone model to characterize the ductility of the material, which leads to a unified cohesive zone model which is suitable for both ductile and brittle materials ^[2].

1.10 Standard Test Methods for Delamination

Three major standardization organizations: the American Society for Testing and Materials (ASTM), European Structural Integrity Society (ESIS) and Japanese Industrial Standards (JIS), developed and adopted the standard testing procedures. The ESIS has developed standards for fracture testing of polymers, including a Kc standard at the ISO voting stage, J-integral test, peel testing, impact testing of polymers and adhesive tests. The standard test like Double Cantilever Beam test, End Notch Flexure test and Mixed-Mode Bending test are explained and expression to obtain the fracture toughness of the material is derived.

1.10.1 DCB Test

The DCB test is mostly used to measure the mode I fracture toughness ^[65]. There are different methods which include a pre-crack in the specimen and without pre-crack. To develop a pre-crack 80% of load will be applied in a lower frequency so that there will be no undesirable premature failure. The crack propagation will be monitored using 1 to 5mm guide marks on the side of the specimen and a load-displacement plot will be generated.

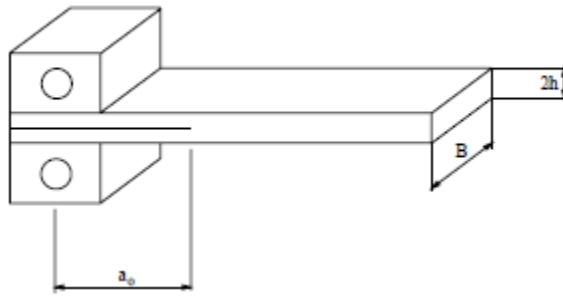


Fig1.10a: DCB Specimen

The strain energy release rate is given by the below expression:

$$G_{Ic} = \frac{P^2 a^2}{hEI}$$

Where P is the applied load, a is measured crack length and E is the Young's modulus and I is moment of inertia.

1.10.2 ENF Testing

The geometry of the specimen is similar to DCM test. The specimen will be placed on a 3-point bending fixture with a half-span length. Testing speed will be 1mm/min and load-displacement curve was obtained for mode II critical strain energy release rate [65].

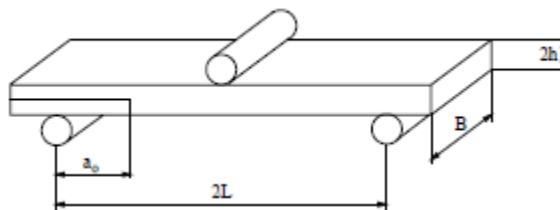


Fig1.10b: ENF Specimen

Based on Direct Beam Theory, for which expression is given as

$$G_{IIc} = \frac{3P^2 a^2}{64hEI}$$

Where P is the applied load, a is measure crack length, h is thickness of specimen, E- Young's modulus and I is moment of inertia.

The above said standard testing methods can be used in evaluation of specimens in laboratory testing methods. Materials manufactured after optimization of properties

through simulation techniques can be evaluated by these testing methods. Physical testing of materials is always time consuming and sophisticated, getting exact results and locating the stress concentration area are complicated. These drawbacks calls for an efficient modelling technique which can serve as a qualitative input in modelling experiments. Modelling can provide better details in achieving best results through experiments.

Chapter - 2

2.0 Cohesive Zone Modelling with ANSYS

The debonding analysis in ANSYS, simulates the separation of bonded contact. It can be used to simulate interface delamination where the interface is modelled using bonded contact with the augmented Lagrangian method or pure penalty method. A cohesive zone material must be used to define the traction separation behaviour of the interface. This analysis can be done with contact element Types like CONTA171, CONTA172, CONTA173, CONTA175, CONTA176 and CONTA177 [66].

The cohesive zone model consists of a constitutive relation between the traction T acting on the interface of material and the corresponding interfacial separation δ . The definitions of traction and separation depend on the element and the material model. The debonding can be modelled in ANSYS in two ways:

2.1 Interface Elements

For interface elements, the interfacial separation is defined as the displacement jump δ , i.e., the difference of the displacement of the adjacent interface surface:

$$\delta = U^{Top} - U^{Bottom} = \text{interfacial separation}$$

The normal of the interface is denoted as local direction n , and the local tangent direction is denoted as t , as shown in Fig9 (Undeformed & Deformed) therefore:

$$\text{Normal Separation, } \delta_n = n \cdot \delta$$

$$\text{Tangential Separation, } \delta_t = t \cdot \delta$$

The interface elements are available for 2D and 3D models according to the nodes, like

- INTER202 – 2D - 4NODE COHESIVE
- INTER203 – 2D – 6NODE COHESIVE
- INTER204 – 3D – 16NODE COHESIVE
- INTER205 – 3D – 8NODE COHESIVE

These elements can be modelled with structural loads along with nodal or element temperature loads.

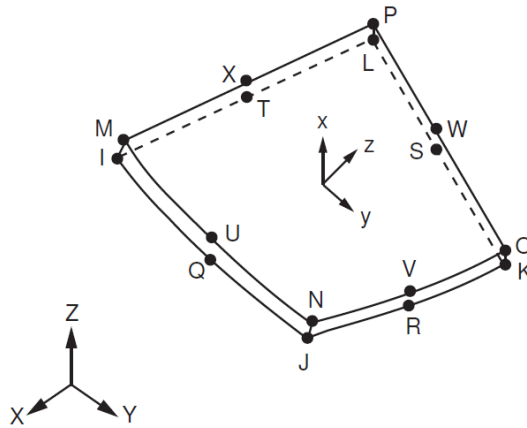


Fig2.1: INTER204 – 16NODE COHESIVE ELEMENT

2.1.1 Contact Elements

Analysis of delamination with contact elements is quite simple, can be used directly with the existing model with including few parameters. Debonding with contact elements has the following advantages over delamination with interface elements ^[66].

- Parts forming the interface can be meshed independently
- Existing models with contact definitions can be easily modified for debonding
- Standard contact and debonding can be simulated with the same contact definitions
- Debonding can be used for various applications; for example, delamination, spot weld failure and stitch failure

This method of delamination, using contact elements is used in all parts of this research. Debonding can be defined in all models that included surface-surface (CONTA171 – 174), node-surface (CONTA175), line-line (CONTA176) and line-surface (CONTA177). To enable debonding in a contact pair, the following contact options must be enabled for the contact element

- Augmented Lagrangian Method or Pure Penalty Method (Keyopt(2)= 0 or 1)
- Bonded Contact (Keyopt(12) = 2,3,4,5 or 6)

Also the material model according to material data, the CZM with bilinear behaviour should be configured to enable delamination. There are two bilinear material models available

- Bilinear material behaviour with traction and separation distance (TB, CZM command with TBOPT=CBDD)
- Bilinear material behaviour with tractions and critical fracture energies (TB, CZM command with TBDATA=CBDE)

2.2 Debonding Modes

We assume that the interface layer between two material/elements is very thin to be considered as negligible.

Mode I Debonding

Mode I debonding defines a mode of separation of the interface surfaces where the separation normal to the interface dominates the slip tangent to the interface. The graph between the normal contact stress and contact gap behaviour shows a linear elastic loading (OA) and a linear softening (AC). The maximum normal contact stress is achieved at a point A. Debonding begins at maximum stress, point A, and is completed at point C while the normal contact stress reduces to zero. The area under the curve (OAC) is the energy released due to debonding. This energy is known as the critical fracture energy. The slope of the line OA determines the contact gap at the maximum normal contact stress and this helps in determining the reduction in contact distance by normal contact stress. This shape of curve characterizes the fracture as brittle or ductile. After initiation of debonding, it is assumed to be cumulative. Any further loading and unloading occurs in a linear elastic manner along line OB.

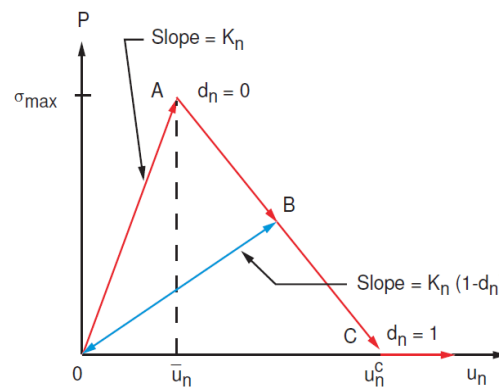


Fig2.1: Material Model – Bilinear Behaviour

The equation for the curve OAC can be written as

$$P = K_n U_n (1 - d_n)$$

Where P- Normal contact stress (In tension), K_n - normal contact stiffness, U_n - contact gap, \bar{U}_n - contact gap at the maximum normal contact stress, U_n^c - contact gap at the completion of debonding, d_n - debonding parameter. The debonding parameter for mode I debonding is expressed as

$$d_n = \left(\frac{U_n - \bar{U}_n}{U_n} \right) \left(\frac{U_n^c}{U_n^c - \bar{U}_n} \right)$$

Therefore the normal critical fracture energy is calculated with the below expression

$$G_{cn} = 1/2 \sigma_{max} U_n^c$$

Where σ_{max} - maximum normal contact stress

For mode I, the tangential contact stress and tangential slip behaviour follows the normal contact stress and contact gap behaviour, which is expressed as

$$\tau_t = K_t U_t (1 - d_n)$$

Where τ_t - tangential contact stress, K_t -tangential contact stiffness, U_t -tangential slip distance

Mode II Debonding

Mode II debonding defines a mode of separation of the interface surfaces where tangential slip dominates the separation normal to the interface. The expression for the tangential contact stress and tangential slip distance behaviour is

$$\tau_t = K_t U_t (1 - d_t)$$

The debonding parameter for mode II is given as

$$d_t = \left(\frac{U_t - \bar{U}_t}{U_t} \right) \left(\frac{U_t^c}{U_t^c - \bar{U}_t} \right)$$

In 3D stress state an isotropic behaviour is assumed and the debonding parameter is computed using an equivalent tangential slip distance.

$$U_t = \sqrt{U_1^2 + U_2^2}$$

Where U_1 and U_2 – slip distance in the two principal directions in the tangent plane. They have individual tangential components.

The tangential critical fracture energy is expressed as

$$G_{ct} = 1/2 \tau_{max} U_t^c$$

Where τ_{max} - maximum tangential contact stress

The normal contact stress and contact gap behaviour follows the tangential contact stress and tangential slip behaviour:

$$P = K_n U_n (1 - d_t)$$

Mixed Mode Debonding

In mixed mode debonding the interface separation depends on both normal and tangential components. The equation for the normal and the tangential contact stresses are expressed as;

$$P = K_n U_n (1 - d_m)$$

And

$$\tau_t = K_t U_t (1 - d_m)$$

The debonding parameter is calculated as follows

$$d_m = \left(\frac{\Delta_m - 1}{\Delta_m} \right) \chi$$

Where

$$\Delta_m = \sqrt{\Delta_n^2 - \Delta_t^2}$$

$$\chi = \left(\frac{U_n^c}{U_n^c - \bar{U}_n} \right) = \left(\frac{U_t^c}{U_t^c - \bar{U}_t} \right)$$

The constraint on χ that the ratio of the contact gap distances be the same as the ratio of tangential slip distances is enforced automatically by appropriately scaling the contact stiffness values. For mixed mode debonding both normal and tangential contact stresses contribute to the total fracture energy and debonding is completed before the critical fracture energy values are reached for the components. Therefore, a power law based energy criterion is used to define the completion of debonding.

$$\left(\frac{G_n}{G_{cn}} \right) + \left(\frac{G_t}{G_{ct}} \right) = 1$$

Where

$$G_n = \int P dU_n$$

$$G_t = \int \tau_t d U_t$$

Are, respectively the normal and tangential fracture energies.

2.3 Material Model – Bilinear Behaviour

2.3.1 Bilinear Material Behaviour with Tractions and Separation Distances

This is a linear elastic material behaviour with linear softening characterized by maximum traction and maximum separation. To define this material in ANSYS APDL, the command:

TB, CZM, 1, 2, ,CBDD

TBDATA, 1, C1,C2,C3,C4, ,

Table 2.3: Description of Bilinear Material Behaviour with Tractions and Separation Distances

CONSTANT	SYMBOL	DESCRIPTION
C1	σ_{max}	Maximum normal contact stress
C2	U_n^c	Contact gap at the completion of debonding
C3	τ_{max}	Maximum equivalent tangential contact stress
C4	$, U_t^c$	Tangential slip at the completion of debonding
C5	η	Artificial damping coefficient
C6	β	Flag for tangential slip under compressive normal contact stress

2.3.2 Bilinear Material Behaviour with Tractions and Critical Fracture Energies

This is a linear elastic material behaviour with linear softening characterized by maximum traction and critical energy release rate. To define this material in ANSYS APDL, the command:

TB, CZM, 1, 2, ,CBDE

TBDATA, 1, C1,C2,C3,C4, ,

Table 2.3: Description of Bilinear Material Behaviour with Traction and Critical Fracture Energies

CONSTANT	SYMBOL	DESCRIPTION
C1	σ_{max}	Maximum normal contact stress
C2	G_{cn}	Critical fracture energy for normal separation
C3	τ_{max}	Maximum equivalent tangential contact stress
C4	G_{ct}	Critical fracture energy for tangential slip
C5	η	Artificial damping coefficient
C6	β	Flag for tangential slip under compressive normal contact stress

2.4 Defining Debonding

Artificial Damping

Debonding is generally accompanied by convergence difficulties in the Newton-Raphson solution. Artificial damping can be used to stabilize the numerical solution. It is activated by specifying the damping coefficient η . The damping coefficient has units of time and should be smaller than the minimum time step size so that the maximum traction and maximum separation values are not exceeded in debonding calculations.

Pinball Radius and Mesh Density

Mesh Density is an important parameter to detect the stress concentrations and stress distribution. Inflation at the contact face can help the solver to converge faster. When using a fine mesh for underlying elements of bonded surfaces, the pinball radius must be increased for that contact elements to ensure that it is greater than the maximum separation value in normal direction. If it is smaller, debonding calculation will be bypassed.

2.5 Solver

2.5.1 Newton-Raphson Method

The Newton-Raphson method is one of the most useful and best known algorithms that relies on the continuity of the function. The finite element discretization process yield a set of simultaneous equations

$$[K]\{U\} = \{F^a\}$$

Where $[K]$ – coefficient matrix, $\{U\}$ – vector of unknown Degree of Freedom values, $\{F^a\}$ – vector of applied loads.

If the coefficient matrix $[K]$ is itself a function of the unknown DOF values, then it becomes a nonlinear equation. The Newton-Raphson method is an iterative process of solving the nonlinear equations and can be written as

$$[K_i^T]\{\Delta U_i\} = \{F^a\} - \{F_i^{nr}\}$$

$$\{U_{i+1}\} = \{U_i\} + \{\Delta U_i\}$$

Where $[K_i^T]$ -Jacobian matrix (tangent matrix), i-subscript representing current iteration, $\{F_i^{nr}\}$ – vector of restoring loads corresponding to the element internal loads

Both $[K_i^T]$ and $\{F_i^{nr}\}$ are evaluate based on the values given by $\{U_i\}$. The difference between the applied load and restoring internal loads is the residual or out-of balance load vector. i.e., the amount the system is out of equilibrium. A single solution iteration is shown in Fig12

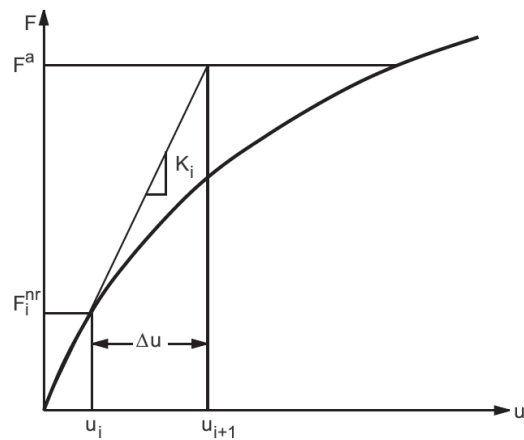


Fig2.5: Newton-Raphson Solution – One iteration

The general algorithm is as follows:

- Assume $\{U_0\}$. $\{U_0\}$, Is usually the converged solution from the previous time step. On the first time step, it is zero.
- Compute the updated tangent matrix $[K_i^T]$ and restoring load $\{F_i^{nr}\}$ from configuration $\{U_i\}$
- Calculate $\{\Delta U_i\}$
- Add $\{\Delta U_i\}$ to $\{U_i\}$ in order to obtain the next approximation $\{U_{i+1}\}$
- Repeat until convergence criteria is obtained

When the stiffness matrix is updated every iteration, the process is termed as full Newton-Raphson procedure. Stiffness matrix could be update less frequently using modified Newton-Raphson procedure.

2.5.2 Convergence

The iteration process continues until convergence criteria is achieved. The maximum number of allowed equilibrium iterations are performed in order to obtain convergence. Convergence is assumed when

$$\|\{R\}\| < \varepsilon_R R_{ref}$$

$$\|\{\Delta U_i\}\| < \varepsilon_U U_{ref}$$

Where $\{R\}$ is residual vector, $\{R\} = \{F^a\} - \{F^{nr}\}$

This is the right-hand side of the Newton-Raphson equation. $\{\Delta U_i\}$ is the DOF increment vector, ε_U and ε_R are tolerances and R_{ref} and U_{ref} are reference values. $\|\ \|\$ is a vector norm, that is a scalar measure of the magnitude of the vector

Convergence therefore, is obtained when size of the residual is less than a tolerance times a reference and/or when the size of the DOF increment is less than a tolerance times a reference value. The default is to use out-of-balance convergence checking only. The default tolerance are 0.001 for both.

2.6 Contact Formulation Algorithms

There are various kinds of contact formulations available in ANSYS. It defines the behaviour of contact and target bodies and prevents/minimizes penetration. To define delamination, it is suitable to use the below algorithms

Augmented Lagrange Method

This method reduces the possibility of ill conditioning of the sub problems that are generated by introducing explicit Lagrange multiplier at each step into the function. It also tends to yield less ill conditioned sub problem and iterates to stay strictly in the feasible region. In structural mechanics, the function is potential energy Π_p that variables are degree of freedom $\{D\}$, and the prescribed relations are multipoint constraints. The unknowns become $\{D\}$ and the Lagrange multipliers ^[67]. To impose constraints by Lagrange multipliers, the constraint equation is multiplied by a row vector containing as many Lagrange multipliers as there are constraint equations. This is expressed as

$$F_n = k_n x_n + \lambda$$

Because of the contact pressure λ , Augmented Lagrange formulation is less sensitive to normal stiffness. Larger the value of the Lagrange multiplier, larger the dividend to relax the constraint or the larger the penalty to tighten the constraint. The advantage is that the original stiffness is not altered when constraints are applied. Therefore constraints can be changed without having to refactor the original stiffness. This property is helpful in problems where different load cases involve different constraints, or in a contact problem where constraints increase in number as the load level increases.

Pure Penalty Method

The objective of the algorithm is to obtain an optimum point of the objective function and satisfying the constraints. Penalty function is designed to quantify this balance and control the algorithm. A sub step will be accepted only if it leads to a sufficient reduction in the penalty function. Whenever a contacting point penetrated normally by an amount, x_n into a target face, it will be pushed back by a normal force, F_n . This is expressed as

$$F_n = k_n x_n$$

Where k_n is called the Normal Stiffness of the contact region. A normal stiffness has no real physical meaning; it is just a numerical parameter of the penalty algorithm. Solution convergence behaviour is usually sensitive to this parameter. A larger k_n usually gives a more accurate solution, but may arise convergence issues. Reducing k_n usually helps convergence, but results in increasing penetration.

If tangential sliding is prohibited, a similar treatment can be implemented. Whenever a contacting point slides tangentially by an amount, it will be pushed back by a tangential force

$$F_t = k_t x_t$$

The simulation settings must be defined carefully to obtain desired results. The above said parameters are of high importance in achieving convergence of the defined finite element simulation. Contact formulation algorithm is of significant importance, because the delamination behaviour depends on this parameter. Solver can be set program defined if the user is not sure of the method, while the software will automatically solve using Newton-Raphson method. Since there will be fracture in the material the convergence of the problem will be quite slow.

Chapter - 3

3.0 Implementation of Cohesive Zone Model

Cohesive zone model is used in analysing the delamination of polymer coated structures. Initially a standard test to measure the tensile shear strength, according to ASTM D1002 ^[68], has been modelled. This model is proven to be working as desired and shows delamination after the critical stress limit. The material properties of the coating material is obtained through manufacturer data sheet and laboratory experiments. Flexural bending test has been done in obtaining and verifying the material data.

The same model has been implemented in real engineering components and structures, to analyse its behaviour in different conditions. Small surface defects has been included in studying the characteristics of coating, which resulted in stress concentration and delamination later. This chapter discusses in detail about all the models developed and their results.

3.1 Obtaining Material Properties

Material data of the polymer coating is obtained from the manufacturer data sheets. The same has been verified in laboratory test. A 3-point bending or flexural strength test has been carried out. The load-displacement characteristics has been plotted and the displacement of the given applied load is also tabulated. This data is used in calculation of Young's Modulus and Flexural Strength of the coating which is used in model as inputs.

Experimental Setup

Three different coating materials are tested and used in the model. Three specimens from each material has been prepared. Specimen of rectangular geometry is prepared and mounted on a 3-point bending test setup.

A Tinius Oleson H25KT tensile testing machine is modified to perform this test. The machine is fitted with a 3-point flexural bending attachment, it has a self-aligning single upper point of contact which is attached to a nose piece, and a lower twin points of contact, one of which is self-aligning and is mounted to the base unit of the machine. The lower twin points of contact have a T-slot variable span. A load cell of 1000N is attached to the loading head. The flexural strength and breaking load is calculated through the software. The data obtained for three materials is plotted below

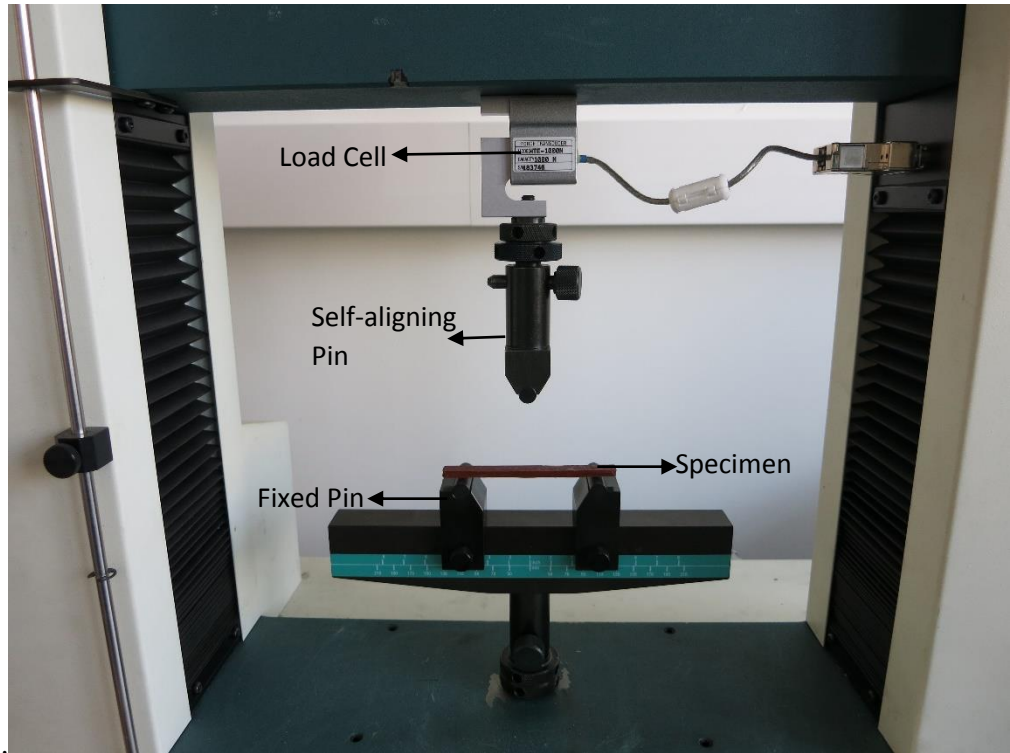


Fig3.2: 3-Point Bending Test of Coating

Specimen 1:

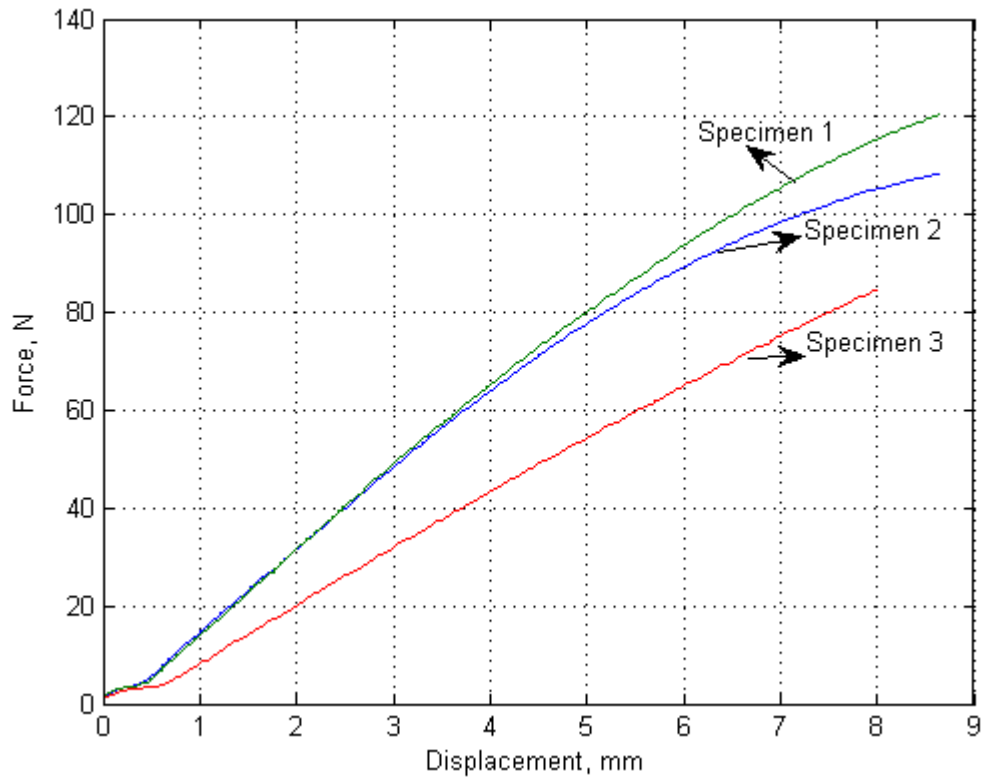


Fig3.2a: Load – Displacement Curve Material 1

Dimensions of Specimens are as below

1. Specimen 1 (l x b x h) = 102.2 x 10 x 3.9
2. Specimen 2 (l x b x h) = 100.7 x 9.6 x 4.2
3. Specimen 3 (l x b x h) = 100.4 x 10.4 x 4.1

The Flexural Young's Modulus and Flexural Strength of this material is analytically calculated using the formula

$$\delta = \frac{FL^3}{48EI} \equiv E = \frac{FL^3}{48\delta I} = 7302 \text{ MPa}$$

$$\sigma_f = \frac{3FL}{2bd^2} = 63.4 \text{ N/mm}^2$$

Where E- Flexural Young's Modulus, δ - deflection, F-Force, L-Length of Specimen, b- width of specimen, d- thickness of specimen.

Specimen 2:

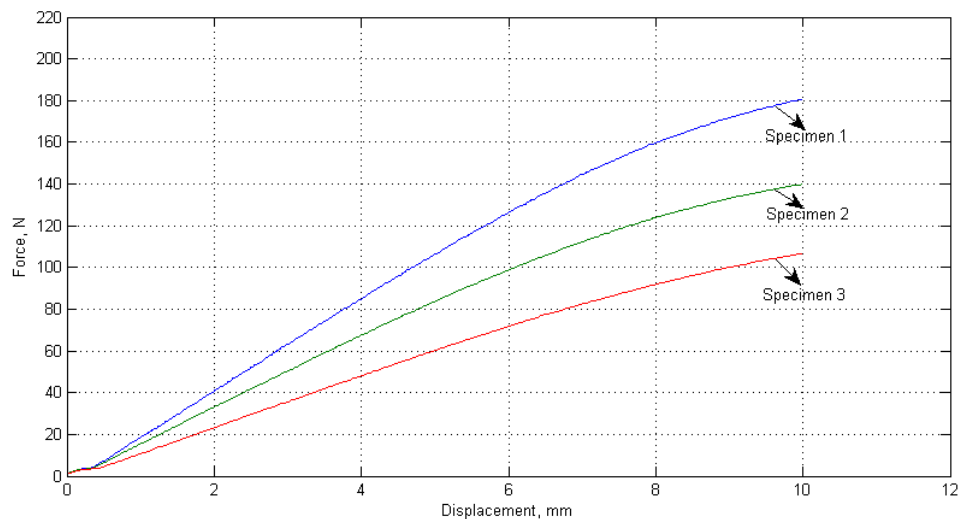


Fig3.2b: Load – Displacement Curve Material 2

Dimensions of Specimens are as below

1. Specimen 1 (l x b x h) = 101 x 10 x 4.9
2. Specimen 2 (l x b x h) = 101.7 x 10.7 x 4.4
3. Specimen 3 (l x b x h) = 101 x 10 x 4.9

Flexural Young's Modulus, E=4227.9 MPa, Flexural Strength = 59.22 MPa

Specimen 3:

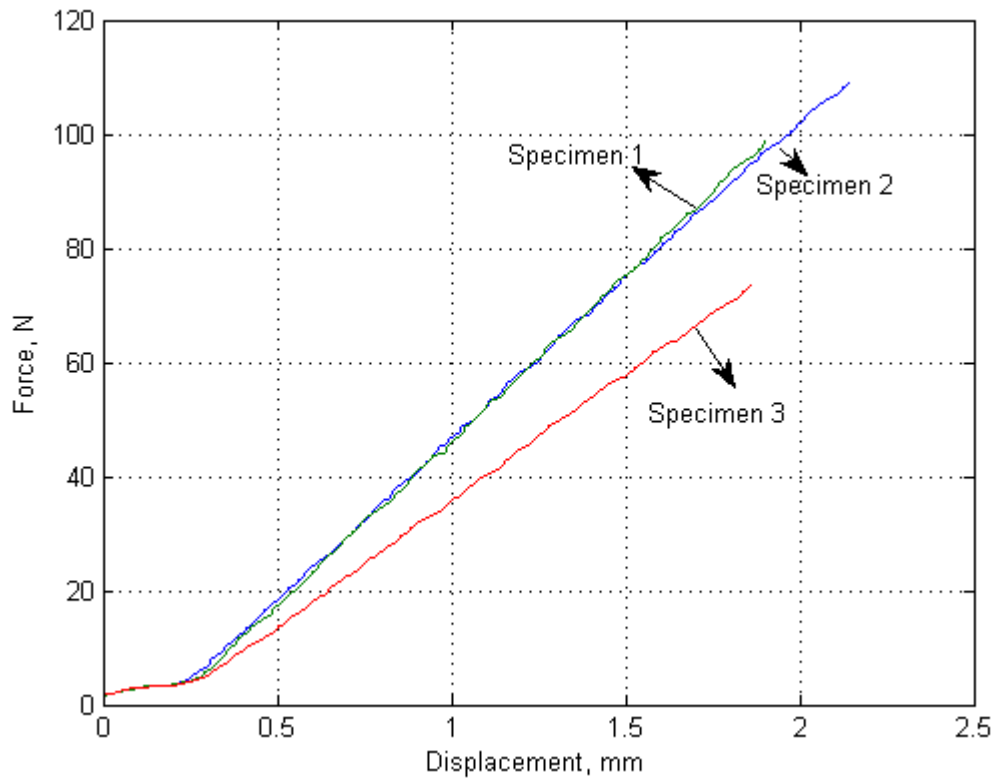


Fig3.2c: Load – Displacement Curve Material 3

Dimensions of Specimens are as below

1. Specimen 1 (l x b x h) = 100.9 x 10 x 4.4
2. Specimen 2 (l x b x h) = 101.5 x 10 x 5
3. Specimen 3 (l x b x h) = 101 x 10.8 x 4.6

Flexural Young's Modulus, $E=20845.78$ MPa, Flexural Strength = 28.03 MPa

The bending test has been performed to obtain the flexural Young's modulus of the coating. This obtained value is used in modelling the coating. The results from the test shows that Material 1 and Material 2 is able to withstand quite high deformation compared to Material 3, also it is more brittle. Voids and surface defects have a significant effect on the performance of coatings.

3.2 Modelling Tensile Shear

A simulation in validating tensile shear strength of the coating is modelled according to ASTM D1002 standard. The plates are coated at the ends of the lap joint. The length of coating is calculated from the expression

$$L = F_{ty}t/\tau$$

$$= 250 * \frac{1.6}{25.5} = 15.686 \text{ mm}$$

Where L- Length of overlap, t – thickness of metal, F_{ty} - yield point of metal, τ - 150% of the estimated average shear strength in adhesive bond

The specimen is designed according the description in the standard, with the below scheme. One end of the plate is fixed while the other has a displacement of 0.1mm. This displacement is select to identify the initiation of delamination. Complete failure will require higher displacement which will have high computation cost and time.

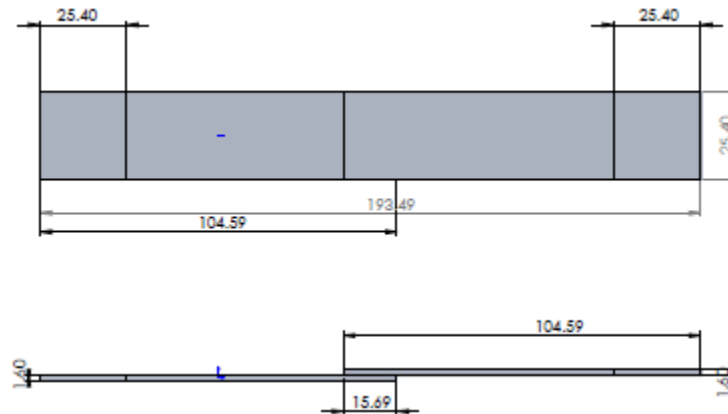


Fig3.2: Configuration of Tensile Shear model

Thickness of Plate	–	1.6mm
Length of Plate	-	104.59mm
Width of Plate	-	25.4mm
Length of Coating	-	15.686mm
Thickness of Coating	-	0.25mm (From Data sheet, DFT of 250 microns for single coat)

3.2.1 Simulation Procedure

The model was developed using Solid works and imported directly to ANSYS Workbench. The plates are assigned as structural steel and adhesive layer with the coating properties. The cohesive zone model with bilinear model using tractions and separation distances technique is used. The Material properties are below

Table 3.2a: Material Properties – Structural Steel

Structural Steel ASME BPV Code, Section 8, Div 2, Table 5-110.1	
Property	Value
Density	7.85e-006 kg mm ⁻³
Young's Modulus MPa	2.00E+05
Poisson's Ratio	0.3
Bulk Modulus MPa	1.67E+05
Compressive Yield Strength MPa	2550
Tensile Yield Strength MPa	250
Tensile Ultimate Strength MPa	460
Shear Modulus MPa	76923

Table 3.2b: Material Properties - Coating

Coating	
Property	Value
Density kg mm ⁻³	1.5
Young's Modulus MPa	4638
Poisson's Ratio	0.25
Bulk Modulus MPa	3092
Tensile Yield Strength MPa	20.96
Tensile Ultimate Strength MPa	30.96
Shear Modulus MPa	1855.2

Table 3.2c: Cohesive Zone Model - Parameters

Cohesive Zone Model	
Parameters	Value
Maximum Normal Contact Stress MPa	17.92
Contact Gap at the Completion of Debonding mm	1.30E-02
Maximum Equivalent Tangential Contact Stress MPa	17.92
Tangential Slip at the Completion of Debonding mm	1.30E-02
Artificial Damping Coefficient s	1.00E-03

Contact Elements

A bonded contact with pure penalty formulation has been defined in both the surface of adhesive and plate.

Meshing

Meshing is the most important parameter in contact debonding to analyse the stress concentration. The adhesive layer is meshed with an element size of 0.12mm and the plate are meshed with element size of 0.4mm.

Fracture mode is included in this analysis with contact debonding. The contact debonding is applied to the contact regions between the coating and plate. The properties of the CZM model is applied to it.

Analysis settings

Analysis settings determine the number of load steps, sub steps and non-linear behaviour of the analysis. This analysis is done with Large Deflections turned ON. Line Search is set to ON, to enhance the convergence of the solver. Newton-Raphson residuals are turned on to analyse the residual force concentrations, in case of non-convergence. A full Newton-Raphson solver is used in solving this analysis.

3.2.2 Results

The results of tensile shear is as below

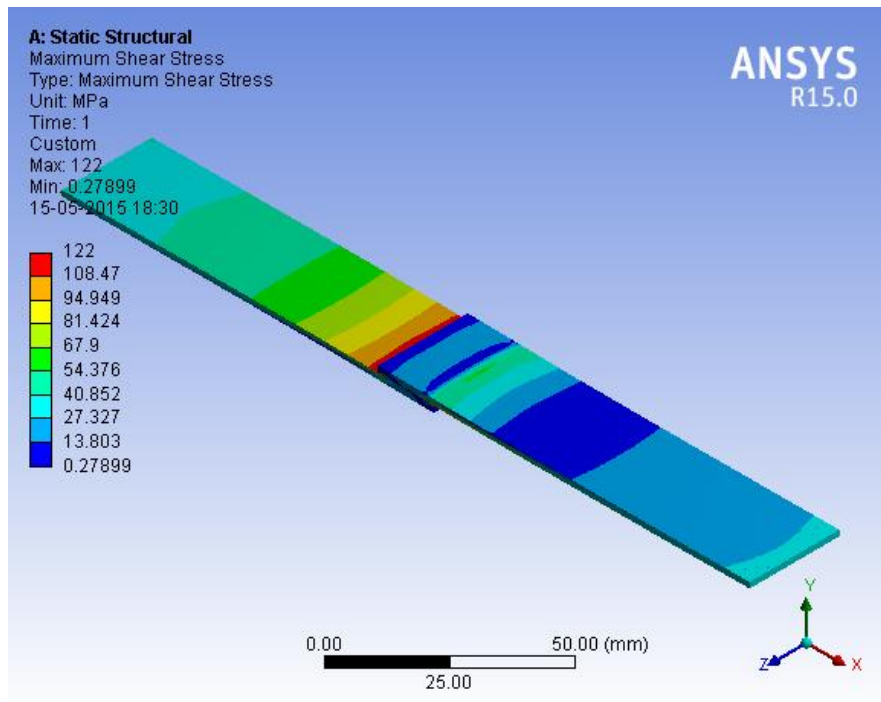


Fig3.2a: Maximum Shear Stress Distribution-Entire Model

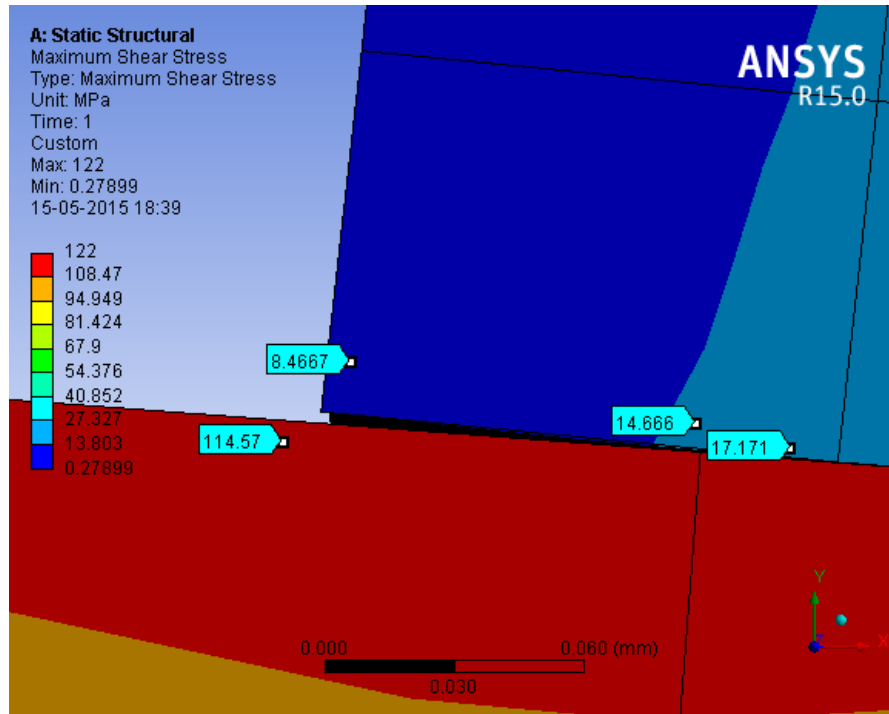


Fig3.2b: Max. Shear Stress - Delamination Initiation

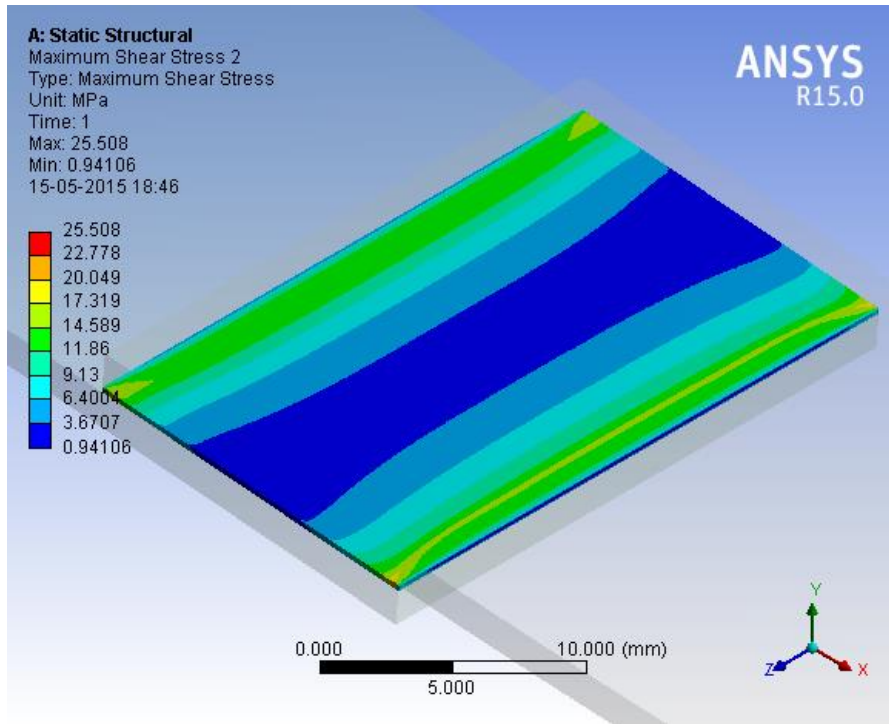


Fig3.2c: Max. Shear Stress Distribution - Coating

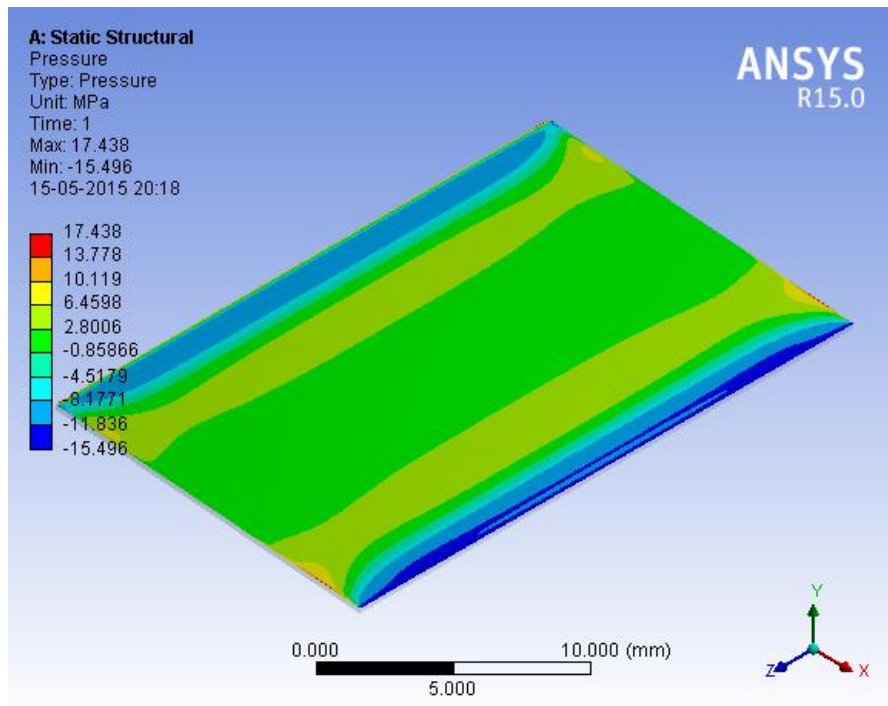


Fig3.2d: Contact Pressure - Coating

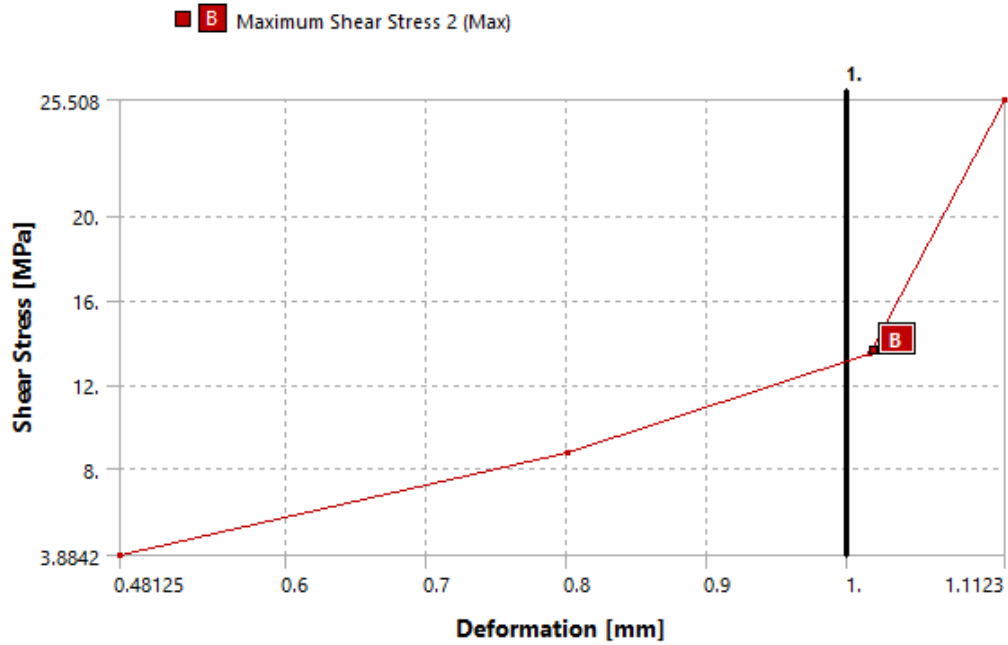


Fig3.2e: Shear Stress – Deformation Plot

3.2.3 Discussion

The results shows that the plate along with the coating as adhesive layer, tries to bend in the tensile load applied to plate. This in turn produces the shear effect on the coating, to evaluate the shear strength of the coating. When the load is applied, the contacting faces of coating and plate is being stressed. This stress is distributed to the coating layer and this gradually increases as the loading continues.

The Maximum Shear Stress distribution on the adhesive layer, shows that, the stress distribution in the ends are higher than the middle of the coating (Fig3.2c). This eventually increases and reaches the critical stress limit. When the maximum normal stress limit of the coating is reached, i.e. 18.116MPa, debonding is initiated (Fig3.2b). From the stress plot, it is also evident that the debonding is initiated at the edges. The top plate, in which the load is applied, tends to push the bottom, fixed plate downwards. This causes the bottom contact layer of coating to delaminate, while the top contacting face, which is in contact with loading plate, also starts to delaminate, due to bending effect.

The Contact Pressure plot (Fig3.2d), the pressure between the plate and the adhesive layer is 17.43 MPa. This later fails even at a lower stress concentration. After delamination of a particular element, the applied load is redistributed to the area that is in contact. The contact surfaces will have stress concentration little higher than the critical limit, due to edge effects, which is plotted in the stress distribution plot.

The graph between the Normal Stress and Deformation of the coating (Fig3.2f), proves the linear behaviour of stress and strain till the critical stress limit. When the critical limit is reached, material softening results in high deformation, at low stress concentration, which leads to complete delamination. The shape of the curve shows a bilinear behaviour during delamination, and the shape of the curve shows a ductile failure because of the steel substrate effect. After, delamination the coating loses its contact with the substrate. The delaminated elements will not have any effect in delamination calculation later. The same behaviour is also seen in the plot between Maximum Shear Stress and Total Deformation of coating layer (Fig3.2e). High deformation is seen after the shear yield point of the material. The comparison between the maximum normal contact stress 18.116 MPa developed in the simulation and maximum delamination stress 17.92 MPa specified by the manufacturer, shows that the model is reliable in analysing delamination.

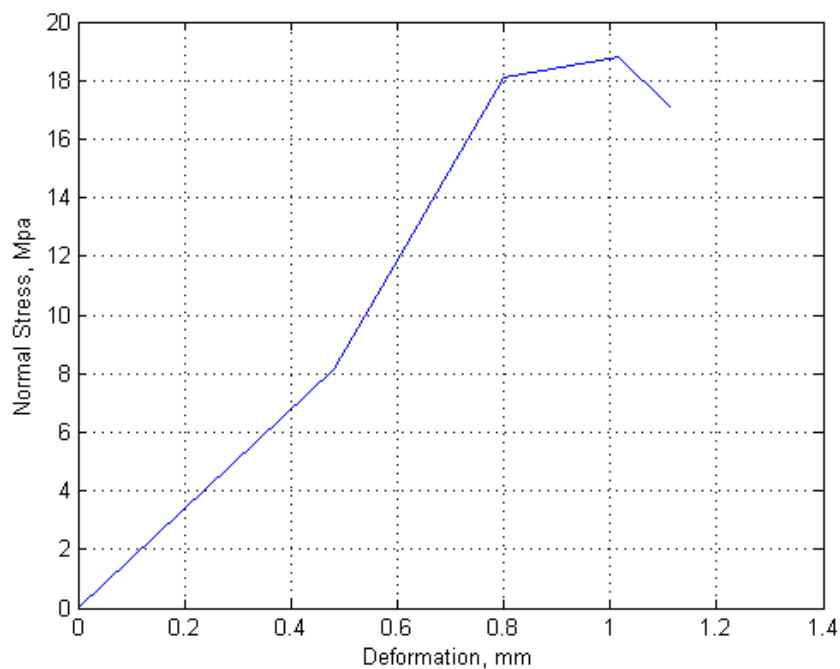


Fig3.2f: Normal Stress – Deformation Plot - Coating

3.4 Delamination in Pipe Structures

The model is reliable in ideal case simulation of lap shear. This model is now implemented to the real engineering structures. Pipes are most critical structures used in transfer of liquids, gases and vapour in various industry. There are various coating available for pipelines according to their application. Pipelines can be coated inside and

outside according to requirement. Inner coating are applied to have a smooth flow, avoid erosion and internal corrosion. Exterior coatings are applied to protect from wear, provide insulation and environmental effects.

Two models have been analysed, one with internal coating and other is with external coating. Both models have a tapping for accessories. Internal pressure load and external load is applied on the pipes and the performance of the coating is studied.

3.4.1 Pipe with External Coating

A section of pipe with a circular hole in it modelled with a layer of polymer coating on top (Fig21). The pipe is assigned the material properties of Grey Cast Iron, while the properties of coating remains the same. There are few changes in cohesive zone model according to the thickness of the coating. The properties are as below. A static load is applied on end, while the other remains fixed.

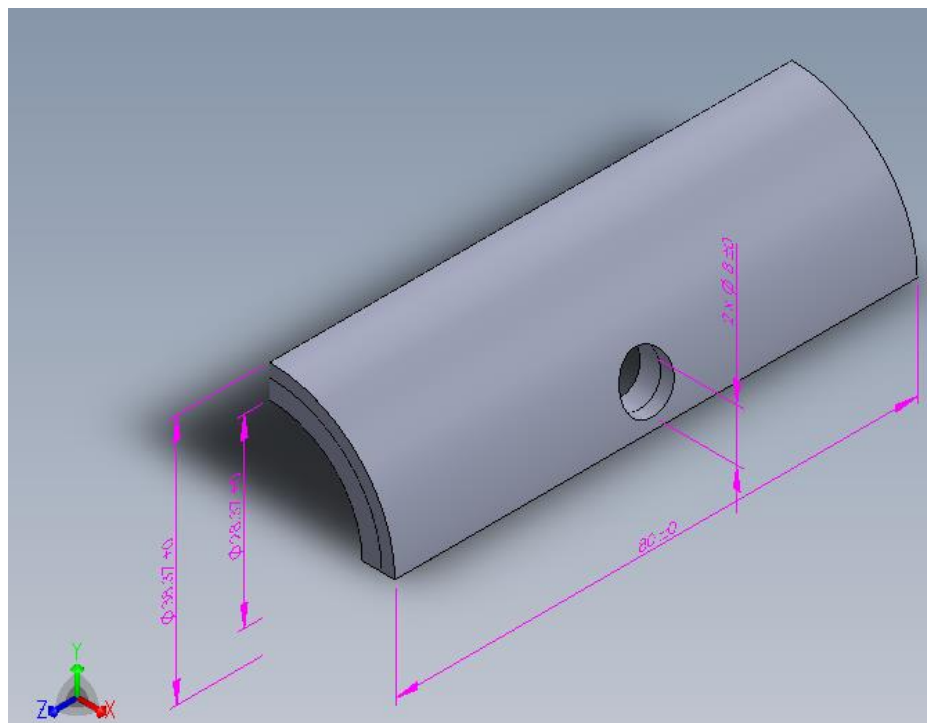


Fig3.4: Section of Pipe with External Coating-Scheme

Table 3.4a: Material Properties – Carbon Steel

Carbon Steel ASTM A106 Grade B ^[69]	
Property	Value
Density kg mm ⁻³	7845
Young's Modulus MPa	2.1E+05
Poisson's Ratio	0.3
Tensile Yield Strength MPa	240
Tensile Ultimate Strength MPa	415

Table 3.4b: Material Properties - CZM

Cohesive Zone Model	
Parameters	Value
Maximum Normal Contact Stress MPa	17.92
Contact Gap at the Completion of Debonding mm	0.01296
Maximum Equivalent Tangential Contact Stress MPa	17.92
Tangential Slip at the Completion of Debonding mm	0.01296
Artificial Damping Coefficient s	1.00E-03

3.4.2 Results

The Normal stress plot of the coating along Y-axis, shows considerable stress concentrations around the circular hole, fixed and loaded edges. This is in agreement with the structural mechanics, which results in stress concentration. The load applied in one end bends the pipe which is fixed at other end, which also causes stress concentration in the fixed end. The contact gap plot, shows that gap between contact and target faces, in the region of stress concentration is quite high. This results in delamination of coating in this load condition. Also there considerable delamination observed in middle of pipe.

The graphical plot of Normal Stress and Normal Strain in the coating, shows that the linear behaviour of the coating, later the coating starts yielding and fails, which cause delamination from the substrate. The stress limit at which yielding occurs here is due

to the effect and resistance offered due to the effect of substrate thickness. The substrate is quite rigid compared to coating, and hence the stress acting on the coating is seen to be higher. Once the substrate starts to deform by the applied load, coating fails immediately due to high stress concentrations.

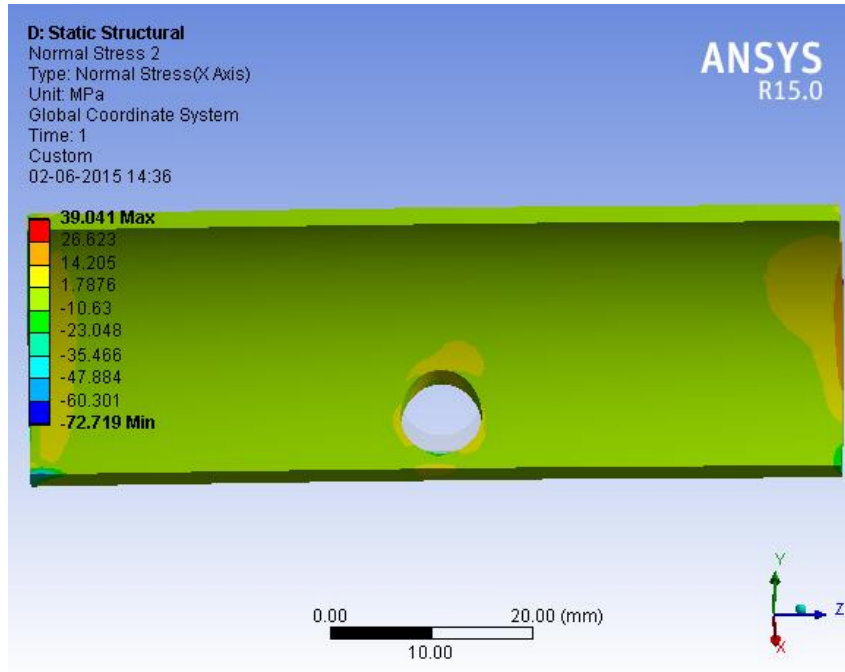


Fig3.4a: Normal Stress Distribution – Coating

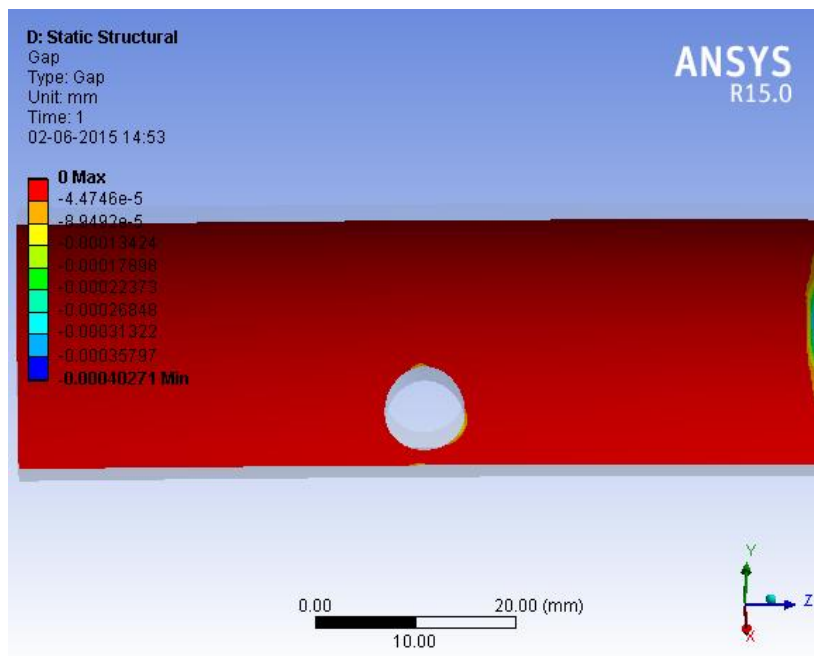


Fig3.4b: Contact Gap - Coating

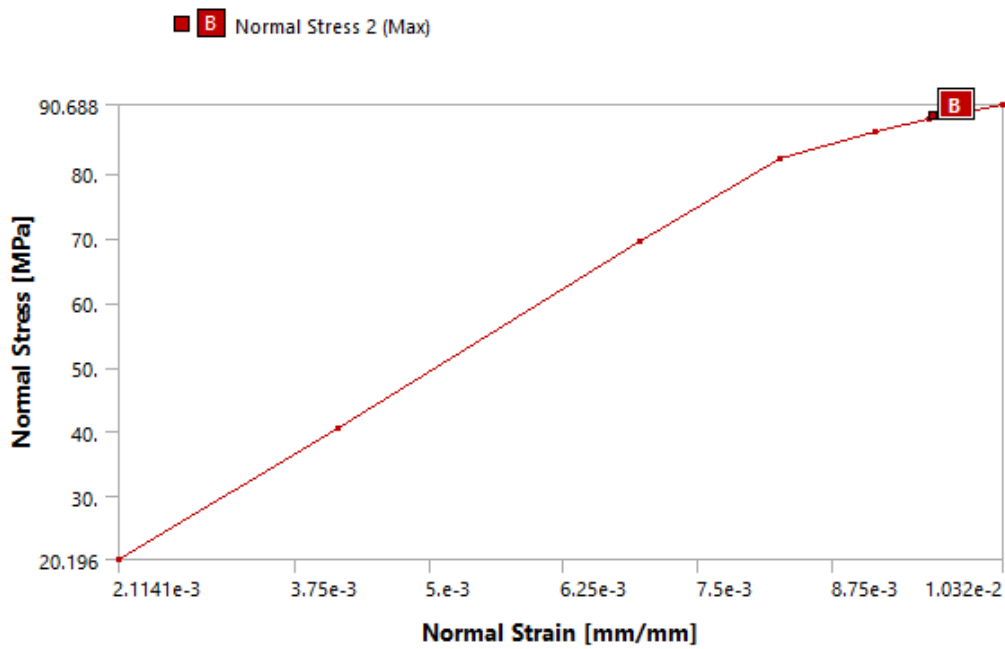


Fig3.4c: Pipe-Normal Stress-Normal Strain Plot

3.4 Pipe with Internal Coating

A model of a Pipe with a T-intersection joint is developed, which is considered to be coated internally. The intersection is considered to be welded to the main pipe. The pipe is assigned the properties of Carbon Steel ASTM A106 Grade B and coating properties remains the same.

The pipe is fixed at one end and other end is free, simulating a continuous pipe. A hydrostatic pressure load is applied to the internal surface of the pipe, the pressure is approximately equal to flow of water inside a pressurized pipe line. The fluid density of water is also specified as an input to simulate the real fluid. A static force is applied on top of the intersection pipe, this load is applied to simulate the structure that is connected to the pipeline. The simulation settings and formulation methods remain unchanged. The results of the simulation is as below

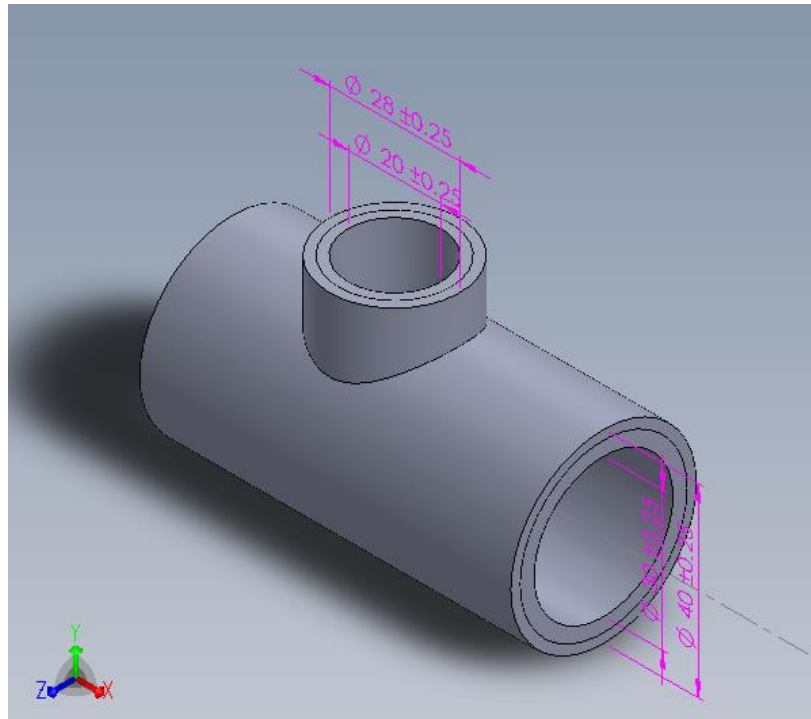


Fig3.4a: Pipe with Internal Coating-Scheme

3.4.4 Results

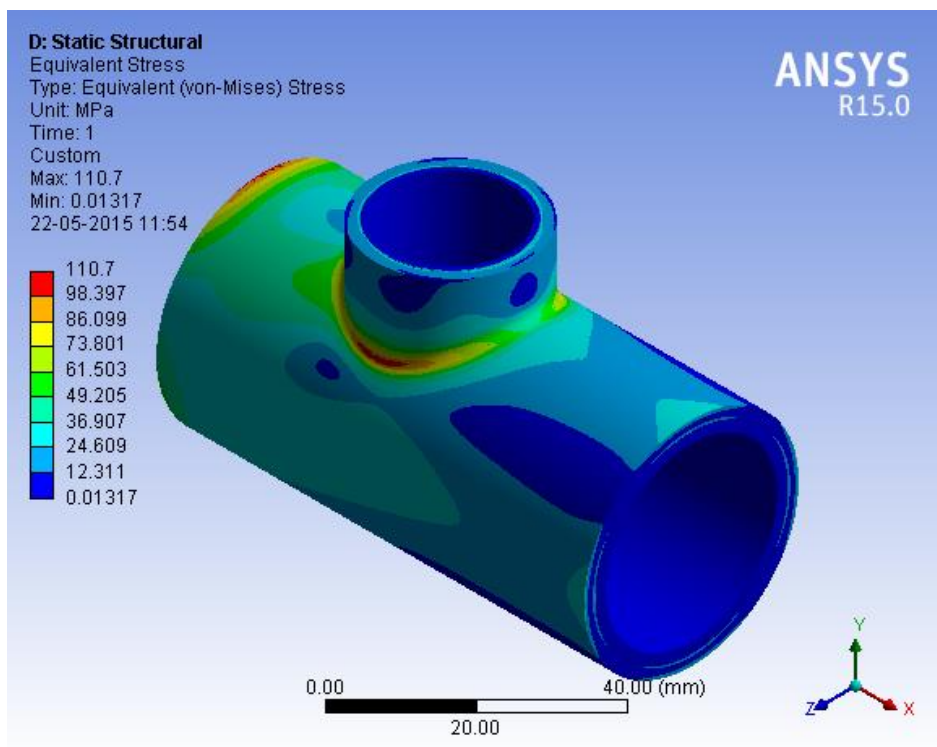


Fig 3.4b: von-Mises Stress Distribution

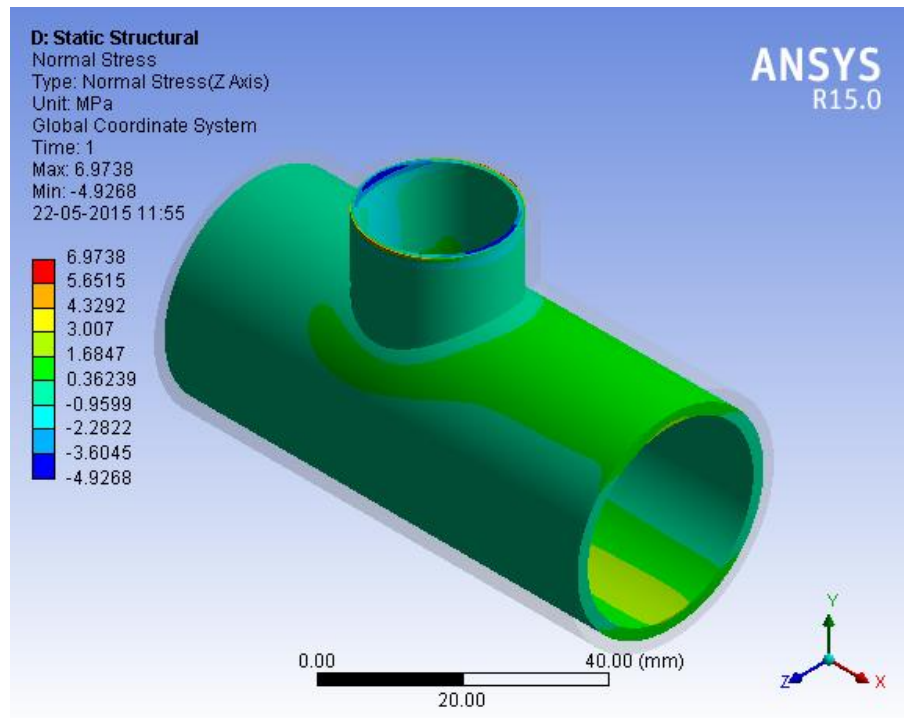


Fig 3.4c: Normal Stress Distribution

The Normal Stress plot of the coating and Equivalent stress plot is taken for comparison of coating performance. The pipe is stresses at the joint of T-intersection, while the coating has not reached its critical failure stress limit. The normal stress distribution of coating also shows that the stress distribution in coating is lower than its critical failure stress limit. This results show that the coating performance is highly depended on the bonded area and applied load.

Though there is minor deformation in the interface region, it is still in contact with the substrate. This is also due to applied loads, i.e. the static load applied on top of the intersection is not as large as the fluid pressure applied on the internal surface. But the distribution also shows the evolving of stress concentration, which may eventually reach the critical limit and lead to delamination or failure. The plot between Normal Stress and Normal Strain of coating also shows a linear relation, which informs us that the coating has not started to yield.

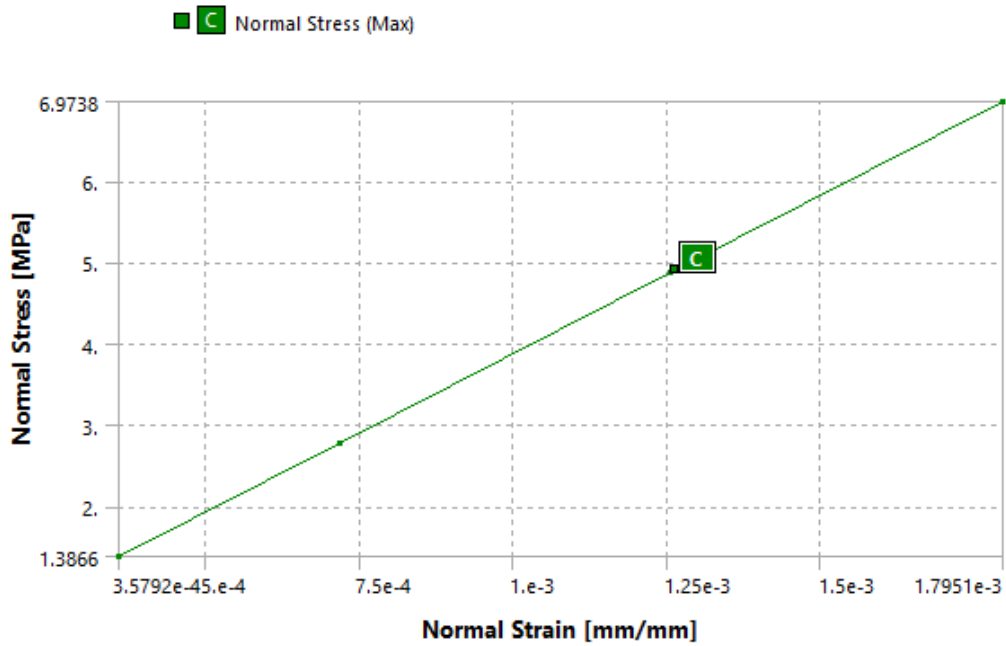


Fig 3.4d: Normal Stress-Normal Strain

3.5 Analysis of Surface Defects

Coatings are also used to extend the span of an equipment or a component. The damaged or defective region is coated with appropriate coating material to put back into service. This application is mostly seen in aircraft maintenance activities. A model to simulate this application is developed

The substrate is configured with properties of 6061 aluminium alloy. The surface is modelled with defects. The defect profile is a shape of inverted rectangle or diamond, the depth of the defect on the substrate is assumed to be 0.2mm. A layer of coating is applied on it and configured with the properties as done earlier. Cohesive Zone Properties are similar to previous cases.

Table 3.5: Material Properties – 6061 Aluminium Alloy

6061 Aluminium Alloy ^[70]	
Property	Value
Density kg mm ⁻³	2770
Young's Modulus MPa	7.1E+05
Poisson's Ratio	0.33
Tensile Yield Strength MPa	280
Tensile Ultimate Strength MPa	310

The model is fixed at one end and a displacement of 3mm is applied on the other. The defects of two sizes are included to study the effect of defect size on the coating performance, it is placed such that the stress concentrations does not affect each other. The scheme of the model is as below

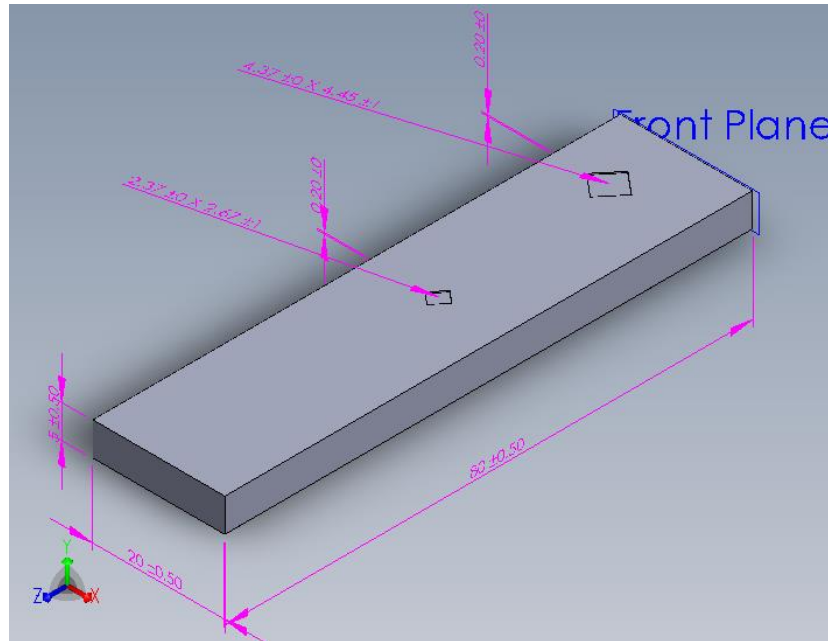


Fig 3.5a: Analysis of Surface Defects on Coating - Scheme

3.5 Results

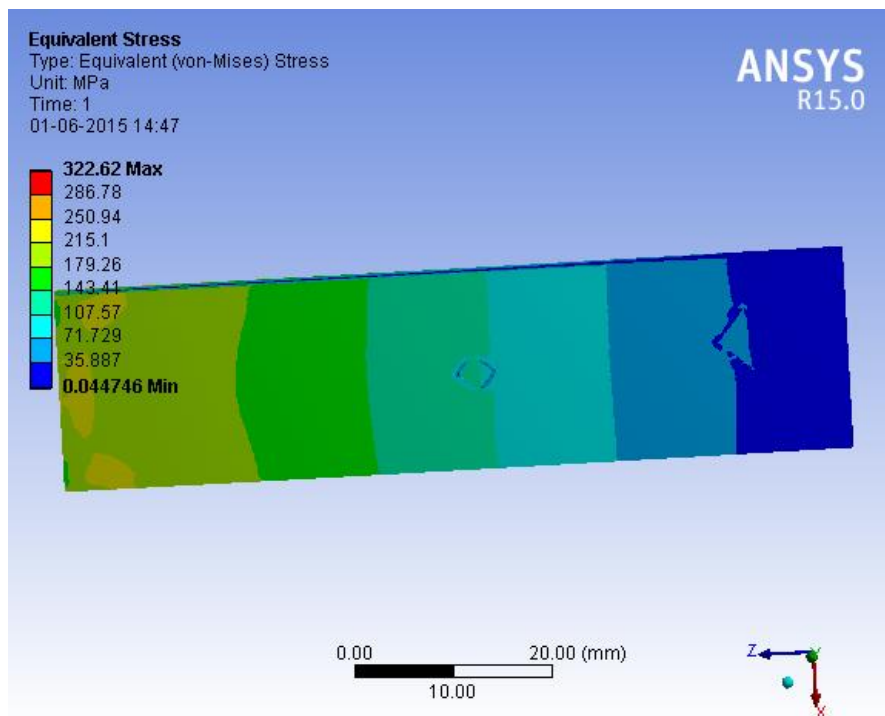


Fig 3.5b: von-Mises Stress Distribution - Substrate

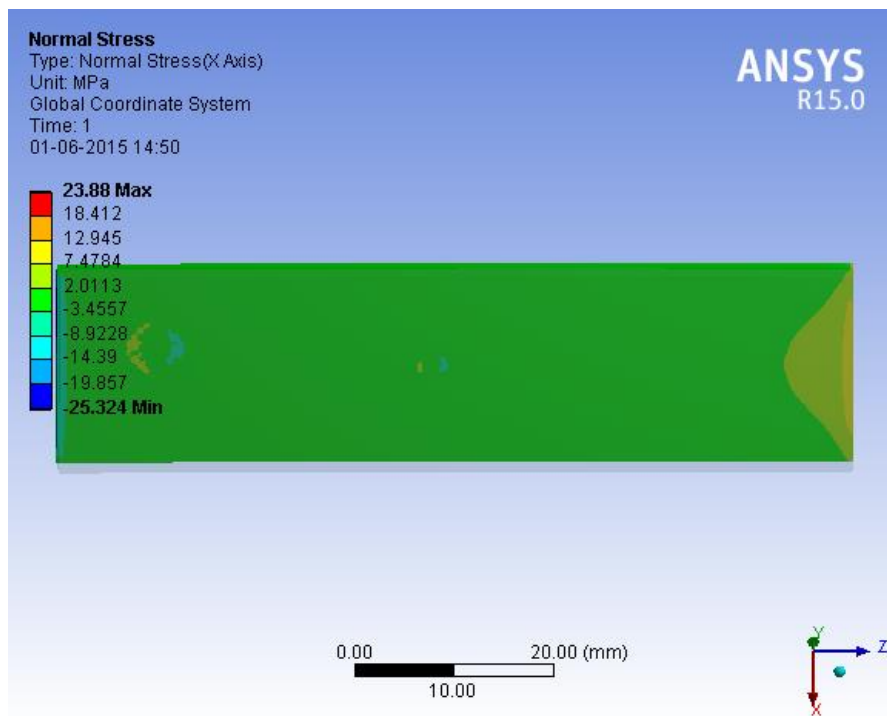


Fig 3.5c: Normal Stress Distribution – Coating

The equivalent stress distribution or von-Mises stress distribution on the Aluminium substrate shows a progressive stress concentration pattern. Significant concentrations can be seen in the edges of the defects. The size of defect also has an importance in the stress concentration pattern. A minor difference in the stress concentration at the edges show the effect of surface defects on the material.

Similarly on the coating, a relatively high stress concentration is observed on the area that covers the defects. The negative compression stress on the edge will result in delamination. There is a positive concentration because of the orientation of applied load. Stress concentration is also observed in the fixed end, the pattern shows a classical bending stress at the middle of the beam. A significant delamination can be observed in the fixed end.

The results shows that the behaviour of the beam with defects under a compressive displacement. The results observed are in agreement with classical mechanics, which shows that the model is realistic and can be applied in analysis of real structures.

Chapter - 4

4.1 Conclusion and Discussions

Analysis of delamination in coated structures, through Finite Element Methods and Fracture Mechanics approach has been done through simulation method. The aim of this work has been accomplished with

1. Identification of Cohesive Zone Model as a realistic technique in delamination analysis
2. CZM has been implemented in Finite Element Model in combination with Fracture mechanics
3. CZM calculated the delamination in shear loading as 18.116 MPa compared to 17.92 MPa specified by manufacturer
4. CZM has been implemented to analyse delamination behaviour in pipe structures and structures with surface defects

The major advantage of Cohesive Zone Model is that, it does not require an initial crack on the surface as like other conventional methods. A contact based debonding using the maximum tangential stress and separation distance has been proven working on real structures. The testing method, tensile lap shear has been simulated successfully. The delamination eventually occurred at the critical stress limit.

The application of CZM in engineering structures, has proven to be a qualitative simulation. It provides the behaviour of coatings in different conditions. Effects of edges, change in cross-section has been studied. The effect of surface defects are also simulated. The results show a classic behaviour, by simulating stress concentrations at corners of defects and stress concentrations at the fixed end. Delamination occurs at the stress concentration areas which leads to failure of coating. This data can be used in optimizing the coating properties, application methods and surface preparation. It can also provide useful information in developing experimental test to analyse the mechanical properties of coatings. It gives savings in cost of sample preparation and testing cost.

4.2 Future Work

The delamination analysis is vital in development of coatings for various applications. The coatings can be modelled in ANSYS with Cohesive Zone Model and can be test in the required conditions. This analysis can be further developed to study the thermal behaviour of coatings by obtaining the existing thermal properties of the coating. Simulation can help in getting and optimized performance for a specific application. Modelling of surface roughness and surface asperities can also be done in improving the reliability of results provided by simulation. The present simulation is done in ideal bonding condition, which is challenging to achieve in real scenario. Simulation results can be used in designing experiments and validated with actual experimental results.

References

1. C. Christofides, Wear of a thin surface coating: modelling and experimental investigations, *Computational Materials Science*, Volume 25, Issues 1–2, September 2002, Pages 61–72
2. Jinxiang Liu, Jun Li, and Litao Liu, Finite Element Analysis for Brittle and Ductile Fracture Using a Unified Cohesive Zone Model, *Advances in Mechanical Engineering* 2013 5:924070;doi:10.1155/2013/924070
3. G.I. Barenblatt, The Mathematical Theory of Equilibrium Cracks Formed in Brittle Fracture, *Zhurnal Prikladnoy Mekhaniki i Tekhnicheskoy Fiziki*, No. A, 19"1, PP. 3-56.
4. Ever J. Barbero , *Finite Element Analysis of Composite Materials*, by CRC Press, ISBN-13: 978-1-4200-5433-0
5. M.-K. Yeh, L.-B. Fang, Contact analysis and experiment of delaminated cantilever composite beam, *Composites Part B: Engineering*, Volume 30, Issue 4, June 1999, Pages 407–414
6. W.-L. YIN, S. N. SALLAM, and G. J. SIMTSES. "Ultimate axial load capacity of a delaminated beam-plate", *AIAA Journal*, Vol. 24, No. 1 (1986), pp. 123-128, doi: 10.2514/3.9231
7. D. Bruno, Delamination buckling in composite laminates with interlaminar defects, *Journal of Composite Materials* July 199125: 907-929
8. D. Bruno, Delamination failure of layered composite plated loaded in compression, *International Journal of Solids and Structures*, Volume 26, Issue 3, 1990, Pages 313–330
9. Domenico Bruno, Fabrizio Greco, An asymptotic analysis of delamination buckling and growth in layered plates, *International Journal of Solids and Structures* 37 (2000) 6239-6276
10. K-F Nilsson, L.E. Asp, Delamination bucking and growth for delaminations at different depths in slender composite panel, *International Journal of Solids and Structures*, Volume 38, Issue 17, April 2001, Pages 3039–3071
11. H. Chai and C.D Babcock, Two-Dimensional modeling of compressive failure in delaminated laminates, *Journal of Composite Materials* (ISSN 0021-9983); 19; 67-98

12. J.D. Withcomb and K.N. Shivakumar, Strain-Energy release rate analysis of plates with postbuckled delaminations, *Journal of Composite Materials* July 1989 vol. 23 no. 7 714-734
13. W.J. Bottega A Growth law for propagation of arbitrary shaped delaminations in layered plates, *International Journal of Solids and Structures*, Volume 19, Issue 11, 1983, Pages 1009-1017
14. B. Storåkers and B. Andersson Nonlinear plate theory applied to delaminations in composites, *Journal of Mechanics and Physics of Solids*, Volume 36, Issue 6, 1988, Pages 689-718
15. J.M Comiez, A.M. Waas and K.W. Shahwan, Delamination buckling: Experiment and Analysis, *International Journal of Solids and Structures*, Volume 32, Issues 6-7, March-April 1995, Pages 767-782
16. G.A. Kardomateas, Postbuckling characteristics in delaminated Kevlar/Epoxy laminates: A Experimental study, *Journal of Composites Technology and Research*, Volume 12, No. 2, Summer 1990, Pages 85-90
17. O. Allix and A. Corigliano, Modeling and Simulation of Crack Propagation in Mixed mode interlaminar fracture specimens, *International Journal of Fracture*, Volume 77, Issue 2, 1996, Pages 111-140
18. D. Bruno and F. Greco, Delamination in composite plates: Influence of shear deformability on interfacial debonding, *Cement and Concrete Composites*, Volume 23, Issue 1, February 2001, Pages 33-45
19. J.W. Hutchinson and Z. Suo, Mixed mode cracking in layered materials, *Advances in Applied Mechanics*, Volume 29, 1991, Pages 63-191
20. N. Point and E. Sacco Delamination of Beam: An Application to the DCB specimen, *International Journal of Fracture*, Volume 79, Issue 3, 1996, Pages 225-247
21. J.G Williams, On the calculation of energy release rate for cracked laminates, *International Journal of Fracture*, Volume 36, Issue 2, February 1988, Pages 101-119
22. G. Alfano and M.A. Crisfield, Finite Element Interface Models for the delamination analysis of laminated composites, *International Journal for Numerical Methods in Engineering*, Volume 50, Issue 7, 10 March 2001, Pages 1710-1736
23. Debonding Giulio Alfano, Silvio de Barros, Laurent Champaney, Comparison between two cohesive-zone Models for the analysis of interface

24. G. Alfano and M.A Crisfield, Solution strategies for the delamination analysis based in a combination of local-control arc-length and line searches, *International Journal for Numerical Methods in Engineering*, Volume 58, Issue 7, 21 October 2003, Pages 999-1048
25. G.I. Barenblatt, The mathematical theory of equilibrium cracks formed in brittle fracture
26. Yielding of steel sheets containing slits D.D. Dugdale
27. M.J van den Bosch and P.J.G. Schreurs ,An improved description of the exponential Xu and Needleman cohesive zone law for mixed mode decohesion, *Engineering Fracture Mechanics*, Volume 73, Issue 9, June 2006, Pages 1220-1234
28. J. Llu, C. Xiang and H.Yuan, Prediction of 3D small fatigue crack propagation in shot-peened specimens, *Computational Materials Science*, Volume 46, Issue 3, September 2009, Pages 566-571
29. J. Llu, H. Yuan and R. Liao, Prediction of fatigue crack growth and residual stress relaxations in shot-peened material, *Materials Science and Engineering: A*, Volume 527, Issue 21-22, 20 August 2010, Pages 5962-5968
30. X.O. Xu, A. Needleman and F.F. Abraham, Effect of inhomogeneities on dynamics crack growth in an elastic solid, *Modelling and Simulation in Materials Science and Engineering*, Volume 5, Issue 5, September 1997 489 doi:10.1088/0965-0393/5/5/005
31. O. Miller, L.B. Freund and A. Needleman, Energy dissipation in dynamic fracture of brittle materials *Modelling and Simulation in Materials Science and Engineering*, Volume 7, Issue 4, July 1999 573 doi:10.1088/0965-0393/7/4/307
32. A. Hilerborg, M. Modeer and P.E. Petersson, Analysis of crack formation and crack growth in concrete by means of fracture mechanics and finite elements, *Cement and Concrete Research*, Volume 6, Issue 6, November 1976, Pages 773-781
33. A. Needleman, A continuum model for void nucleation by inclusion debonding, *Journal of Applied Mechanics*, Volume 54, Issue 3, 01 September 1987, Pages 525-531
34. A. Needleman, An analysis of decohesion along an imperfect interface , *International Journal of Fracture*, Volume 42, Issue 1, January 1990, Pages 21-40

35. H. Yuan, G. Lln and A. Cornec, Verification of a cohesive zone model for ductile fracture, *Journal of Engineering Materials and Technology*, Volume 118, Issue 2, 01 April 1996, Pages 192-200
36. P.H. Geubelle and J.S. Baylor, Impact-induced delamination of composites: a 2D simulation, *Composited Part B: Engineering*, Volume 29, Issue 5, September 1998, Pages 589-602
37. V. Tvergaard and J.W. Hutchinson, The relation between crack growth resistance and fracture process parameters in elastic-plastic solids, *Journal of the Mechanics and Physics of Solids*, Volume 40, Issue 6, August 1992, Pages 1377-1397
38. J.L. Chaboche, R. Girard, On the interface debonding models, *International Journal of Damage Mechanics*, Volume 6, Issue 3, July 1997, Pages 220-257
39. T.L Anderson, *Fracture Mechanics, Fundamentals and Applications*, by CRC Press, ISBN: 978-0-8493-1656-2
40. A.A. Griffith, *The phenomena of rupture and flow in solids*
41. Irwin G.R , *Onset of fast crack propagation in High Strength steel and aluminium alloys*
42. Ward I.M, *Mechanical properties of solid polymers*, John Wiley & Sons, 2012, ISBN 978-1-4443-1950-7
43. Sternstein S.S *Yield criteria for plastic deformation of glassy high polymers in general stress fields*
44. Westergaard H.M , *Bearing pressures and Cracks*
45. *On the Stress distribution at the base of a stationary crack* Williams M.I
46. *The stress around a fault or crack in dissimilar media* Williams M.I
47. England A.H, *A crack between dissimilar media*, *Journal of Applied Mechanics*, Volume 32, Issue 2, 01 June 1965, Pages 400-402
48. Comninou .M and Schmuser .D, *The interface crack in a combined tension-compression and shear field*, *Journal of Applied Mechanics*, Volume 46, Issue 2, 01 June 1979, Pages 345-348
49. Erdogan .F, *Stress distribution in a nonhomogenous elastic plane with cracks*, *Journal of Applied Mechanics*, Volume 30, Issue 2, 01 June 1963, Pages 232-236
50. *On strain energy release rate in biomaterial media* Sun C.T and Jih C.J
51. Willis J.R, *Fracture mechanics of interfacial cracks*, *Journal of the Mechanics and Physics of Solids*, Volume 19, Issue 6, November 1971, Pages 353-368

52. Wang S.S and Choi .I, The interface crack between dissimilar anisotropic composites under mixed-mode loading, *Journal of Applied Mechanics*, Volume 50, Issue 1, 01 March 1983, Pages 179-183
53. Barnett D.M Asaro R.J, The fracture mechanics of slit-like cracks in anisotropic elastic media, *Journal of the Mechanics and Physics of Solids*, Volume 20, Issue 6, December 1972, Pages 353-366
54. Rabinovitch .O, Debonding analysis of fibre-reinforced-polymer strengthened beams: Cohesive zone modelling versus a linear elastic mechanics approach, *Engineering Fracture Mechanics*, Volume 75, Issue 10, July 2008, Pages 2842-2859
55. Taljsten .B, Strengthening of beams by plate bonding, *Journal of Materials in Civil Engineering*, Volume 9, Issue 4, November 1997, Pages 206-212
56. Mohammadi .S, Discontinuum mechanics by Combine Finite/Discrete elements
57. Belytschko T, Organ .D and Krongauz .Y, A coupled finite element free Galerkin method, *Computational Mechanics*, Volume 17, Issue 3, 1995, Pages 186-195
58. Ghorashi S.S, Valizadeh .N and Mohammadi .S, Extended isogeometric analysis (XIGA) for analysis of stationary and propagating cracks, *International Journal for Numerical Methods in Engineering*, Volume 89, Issue 9, 2 March 2012, Pages 1069-1101
59. Sprenger .W Gruttmann .F and Wagner .W, Delamination growth nalysis in laminated structures with continuum-based 3D-shell elements and a viscoplastic softening model, *Computer Methods in Applied Mechanics and Engineering*, Volume 185, Issue 2-4, 12 May 2000, Pages 123-139
60. Mohammadi .S and Asadpoure .A 3D multi delamination/fracture analysis of composites subjected to impact loadings, *Journal of Composite Materials*, Volume 41, Issue 12, June 2007, Pages 1459-1475
61. Bruno .D, Carpino .R and Greco, Modelling of mixed mode debonding in externally FRP reinforced beams, *Composites Science and Technology*, Volume 67, Issue 7-8, June 2007, 1459-1474
62. Rabinovitch .O, Fracture mechanics failure criteria for RC beams strengthened with FRP strips – a simplified approach, *Composite Structures*, Volume 64, Issue 3-4, June 2004, Pages 479-492
63. Finite element stress analysis of multidirectional laminated composite structures Borovkov ,A, Kiylo .O, et.al

64. P. Davies, B.R. Blackman, A.J. Brunner, Standard Test Methods for Delamination Resistance of Composite Materials: Current Status, Applied Composite Materials, Volume 5, Issue 6, November 1998, Pages 345-364
65. ANSYS Inc., Theory Reference for the Mechanical APDL and Mechanical Applications, Release 12.0, ANSYS Inc., April 2009
66. ANSYS Inc., Contact Technology Guide, Release 12.1, ANSYS Inc., November 2009
67. Rober D. Cook, David S. Markus Michael E. Plesha Robert J. Witt, Concepts and Application of Finite Element Analysis, Fourth Edition, , John Wiley & Sons, 2002, ISBN 978-0-471-35605-9
68. ASTM Standard D1002-01,2001, “Standard Test Method for Apparent Shear Strength of Single-Lap-Joint Adhesively Bonded Metal Specimens by Tension Loading (Metal-to-Metal), ASTM International, West Conshohocken, PA, 2001
69. ASTM Standard A 106/A 106M-04,2004,”Standard Specification for Seamless Carbon Steel Pipe for High-Temperature Service”, ASTM International, West Conshohocken, PA, 2001
70. MIL-HDBK-5H, “Military Handbook-Metallic Materials For Aerospace Vehicle Structures”, Department of Defence, United States of America, 1 December 1998